Training report

Building and characterizing a fluorescence setup to measure very low concentrations of analytes/biomarkers

Submitted by

Nathan Mortiaux

Under the supervision of

Prof. Heidi Ottevaere
and
Dr. Yunfeng Nie

May 2020

Contents

1 Introduction

This training report is the result of my internship in the B-Phot Brussels Photonics team of the VUB that took place between February 3 and April 3, 2020. The project of this internship finds its context in the European SensApp project which regroups several European research institutes and universities, including the VUB. The goal of this project is to develop a method to diagnose the Alzheimer's disease in a faster and non-invasive manner, simply through a blood test, which is currently not possible because the concentration of biomarkers of the Alzheimer's disease in the blood is too low. During this internship, I was lead to build, align and calibrate a fluorescence detection setup. Using this setup, I made measurements of the fluorescence intensity of low concentrations of dye solutions. From those measurements, I performed calculations of the signal to noise ratio in order to determine the limit of detection of the setup. Finally, I studied the kinetics of photobleaching in order to get to a better understanding of its impact on the measurements.

2 Building and improving a fluorescence detection setup

This first section retraces step by step the building process of the setup, starting with a brief description of the components that were used.

2.1 Components

- The dye that we used to prepare our sample was Alexa Fluor™ 647. This dye is characterized by a maximum absorbance at a wavelength of 652 nm and a maximum emission at a wavelength of 672 nm. The absorbance and emission spectrum of Alexa Fluor™ 647 are shown in Figure 1

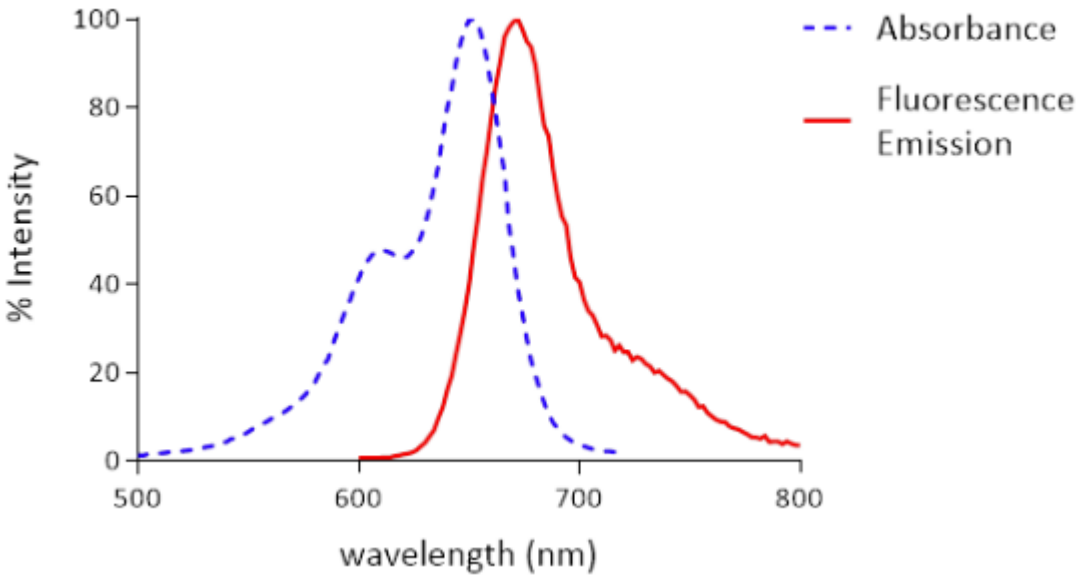

Figure 1: absorbance and emission spectrum of Alexa Fluor™ 647

- The detector we used was a Hamamastu No. H10721-01 photomultiplier tube (PMT) whose gain could be adjusted via a control voltage that can range from 0.5 V to 1.1 V.

- The low voltage input and the control voltage of the PMT were provided by an Agilent E3647A DC power supply.
- The light source was a Thorlabs CPS635F laser diode emitting light at a wavelength of 635 nm
- The emission filter and excitation filter that we used were a Semrock FF01-680/42 and a Semrock FF01-635/18, respectively. Those are both single-band bandpass filters with passing band centered at 680 nm and 42 nm wide for the emission filter, and a passing band centered at 635 nm and 18 nm wide for the excitation filter.
- To attenuate the intensity of the laser, we used a set of absorptive Neutral density filters from Thorlabs with respective optical densities of 0.2, 0.3, 0.4, 0.6, 1.0, and 3.0. The optical density (OD) is related to the transmittance, T by the following equation :

$$OD = log_{10}\left(\frac{1}{T}\right) \tag{1}$$

- The pinholes that were used were precision pinholes from Thorlabs with diameters of 100 µm,200 µm, 400 µm, 600 µm and 800 µm.
- The objective lens that was used was an Olympus Plan N Objective which is an infinity-corrected objective lens with a magnification of 10x and a numerical aperture of 0.25.
- In order to focus the parallel light beam produced by the objective lens on the pinhole, we used a TTL180-A tube lens from Thorlabs, which is a 180mm tube lens with a working distance of 130 mm
- To acquire the data, we used a national instruments NI-9229 Data Acquisition system (DAQ) to record the output voltage of the PMT.

2.2 Finding the working distance of the objective lens

The first step in the building of the setup was to place the objective lens at a fixed position above a Z stage in order to find the position of the Z stage for which a sample placed on it is in focus range of the objective lens. To do so, we placed a CMOS camera behind the objective lens and we used a sample that featured small details, which was a piece of paper printed with small characters. Because we work with an infinity corrected objective lens, we equipped the CMOS camera with a zoom lens focused to infinity. A picture of the setup is shown in figure 2.

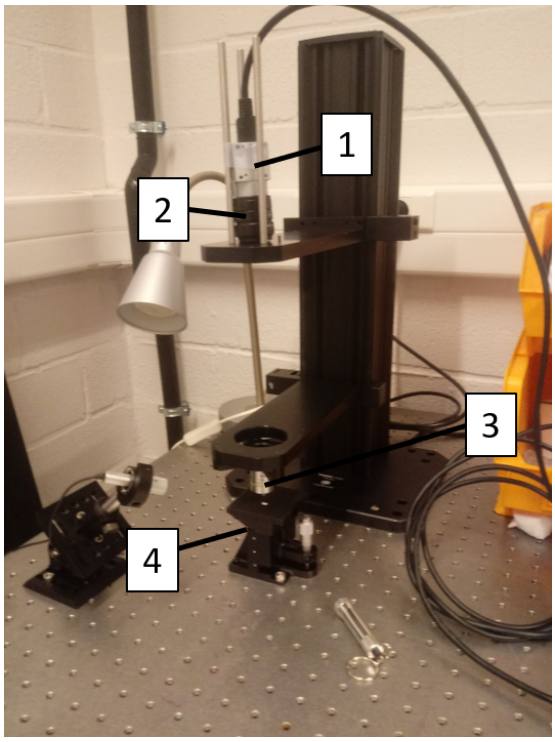

Figure 2: Picture of the setup that was used to find the Z stage position corresponding to the working distance of the objective lens. (1) CMOS camera (2) zoom lens (3) objective lens (4) Z stage .

The experiment consisted in adjusting the position of the Z stage while displaying the image from the CMOS camera on the computer monitor until we got a focused image. Images from the CMOS camera for two different positions of the Z stage are shown in Figure 3. A focused image was obtained when the Z stage micrometer was set to 4.25 mm. Taking into account the thickness of the piece of paper, which was 0.3 mm, we concluded that in order to be at working distance of the objective lens, the Z stage micrometer has to be set to 3.95 mm, value to which the thickness of the sample needs to be added.

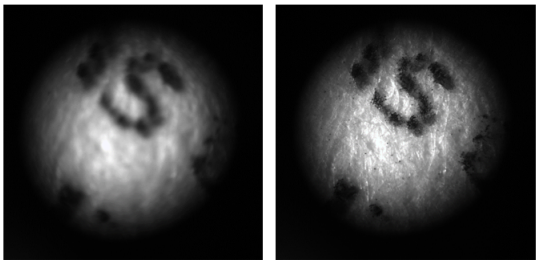

Figure 3: Images from the CMOS camera for two different positions of the Z stage. On the left, the image is unfocused which means that the sample is not in correct working distance from the objective. The image on the right is focused and corresponds to a position of the Z stage set to 4.25 mm.

2.3 placing the pinhole

The next step was to determine the optimal position for the pinhole. To do so, we added the tube lens behind the objective lens and we mounted the 800 µm diameter pinhole on a Z stage. We used a

white piece of paper as a sample in order to scatter the incident light from the laser and we measured the intensity behind the pinhole using a PM100 Digital Power Meter from Thorlabs equipped with a semiconductor sensor. Then, we tried to find a maximum in the intensity measured by the power meter by adjusting the position of the pinhole. The result of this experiment was that we couldn't find a maximum.

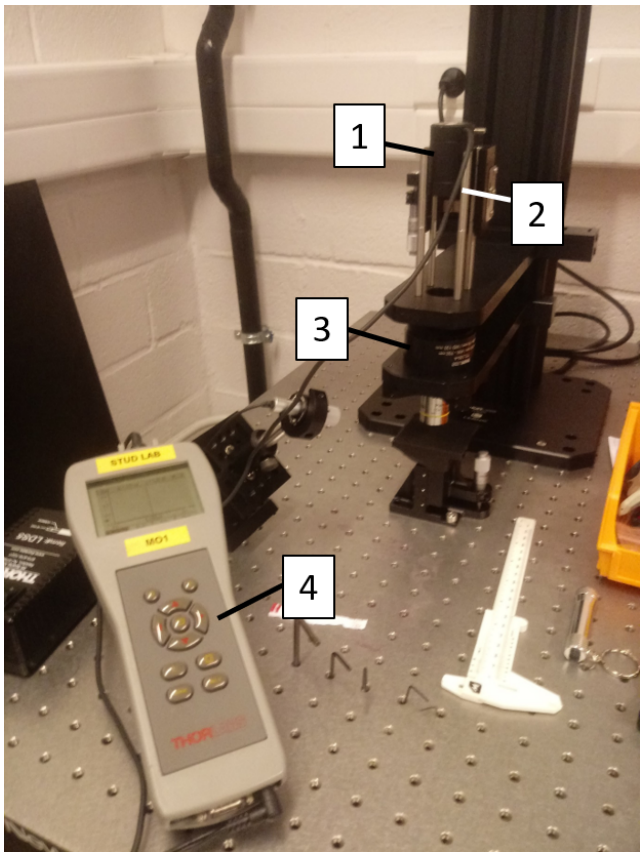

Figure 4: Picture of the setup that was used to find the optimal position of the pinhole. (1) semiconductor sensor (2) pinhole monted on a Z stage (3) tube lens (4) power meter

In fact, the fact that we couldn't find a maximum while adjusting the pinhole position is not surprising. to understand why, we need to look at the optical slice thickness, a quantity that is mostly used in confocal microscopy and which is defined by equation 2. This quantity corresponds to the thickness of the slice of the sample from which the light is focused on the pinhole. [1]

$$\text{Optical slice thickness} = \sqrt{\left(\frac{0.88 * \lambda_{em}}{n - \sqrt{n^2 - NA^2}}\right)^2 \left(\frac{\sqrt{2} n PH}{NA}\right)^2} \tag{2}$$

where λ_{em} is the wavelength of emission, n is the refractive index of the medium, NA is the numerical aperture of the objective lens and PH is the object-side pinhole diameter, in µm, which corresponds to the pinhole diameter divided by the magnification of the objective lens.

Plugging the parameters of our setup into equation (2), we obtain an optical slice thickness of 452.9 µm for a pinhole diameter of 800 µm. Because the axial magnification is equal to the lateral magnification squared, that means the the image of this slice is 100 times larger in the z direction, which is more than 4.5 cm. This explains why a maximum could not be measured by making small adjustments in the

position of the pinhole. The conclusion to this experiment being that since we work with rather large pinholes, we don't need to be extremely precise when placing the pinhole. For this reason we set the pinhole at a fixed position approximately equal to the working distance of the tube lens, which is 130 mm.

2.4 Laser alignment

Once the pinhole position was fixed, we changed the semiconductor sensor for the PMT and connected it to the DAQ as shown in the picture of the setup presented in figure 5.At this point, we also added the emission filter between the objective lens and the tube lens. We then mounted the laser on two stages, placed perpendicularly so we could finely adjust the alignment of the laser by changing its position in the X and Y direction, as shown by the arrows drawn on the picture of the setup in figure 6. The laser focus was adjusted in order to be focused on a sample placed at working distance of the objective lens.

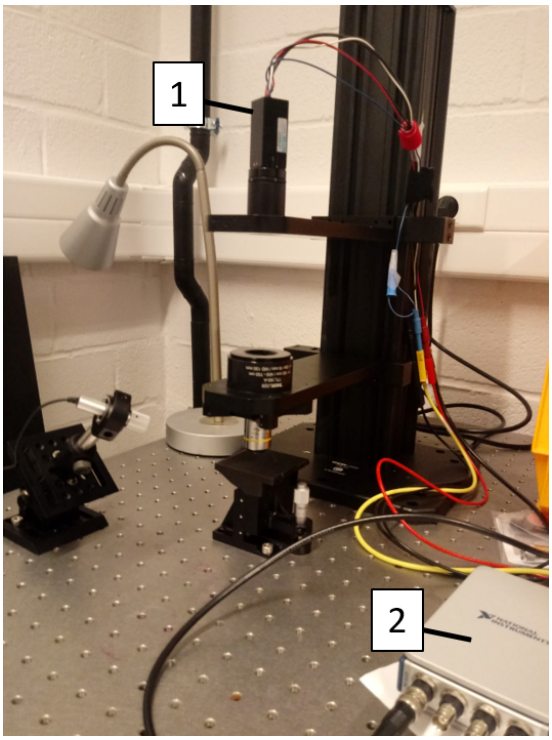

Figure 5: Picture of the setup using the PMT (1) connected to the DAQ (2).

In order to determine the positions of the XY and Z stages that lead to an optimal alignment, we performed measurements using a calibrated fluorescent sample. The positions of the maximum were first roughly determined by eye by monitoring the output signal in real time using DAQExpress while adjusting the positions of the stages. Then, we recorded the output voltage of the PMT for a duration of 1 second, with a rate of 25000 samples per second, adjusting the position of one stage at a time, setting the two other ones to their approximate position of maximum. Those measurements were performed for each available pinhole diameter. Because the fluorescence intensity produced by the calibrated sample was really high, we had to attenuate the intensity of the laser by adding ND filters in front of it when using larger pinholes in order to not damage the PMT. We also adjusted the control voltage depending on the pinhole diameter in order to have enough signal when using smaller pinholes. A typical result from these measurements is shown in Figure 7. This curve was obtained by plotting the mean value of the output voltage as a function of the position of the Z stage. We can clearly see a maximum around

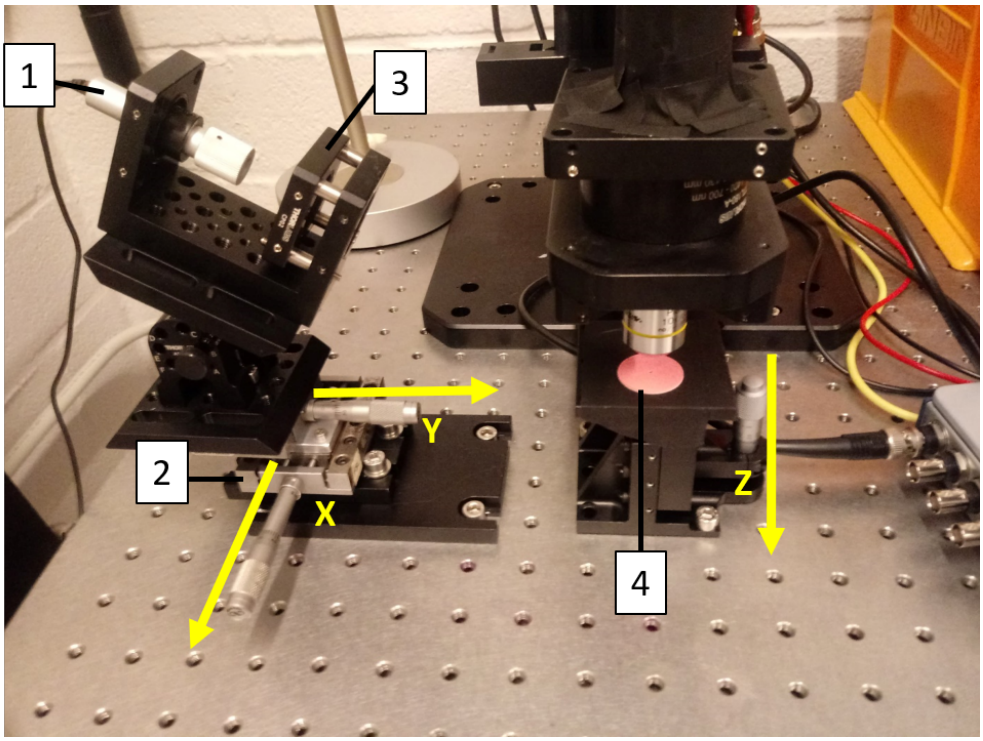

Figure 6: Picture of the setup that was used to determine the position of maximum signal for the X, Y and Z stages. (1) laser (2) XY stage (3) ND filter (4) calibrated fluorescent sample from Thorlabs

4.75 mm. From this data, we measured the position of the maximum and the the 5% tolerance interval in the 3 directions for each pinhole. The results are summarized in Table 1.

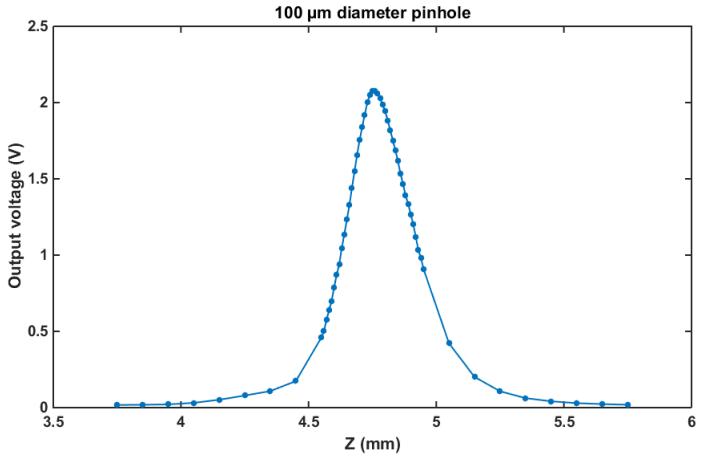

Figure 7: Mean value of the output voltage of the PMT as a function of the position in the Z direction.

Pinhole diameter (µm)	X (mm)	Y (mm)	Z (mm)	Control Voltage (V)	Filter optical density
100	19.36 ± 0.03	7.10 ± 0.05	4.76 ± 0.03	0.7	none
200	19.36 ± 0.02	7.04 ± 0.06	4.73 ± 0.03	0.6	none
400	19.36 ± 0.02	7.06 ± 0.04	4.76 ± 0.03	0.5	none
600	19.36 ± 0.08	4.74 ± 0.12	5.52 ± 0.06	0.8	1.0
800	19.36 ± 0.08	5.94 ± 0.06	4.06 ± 0.05	1.0	3.0

Table 1: Summary of the results for the position of the XY and Z stage leading to a maximum output voltage. the values in the X, Y and Z columns correspond to the position of the maximum ±5% tolerance

First of all, we can see from the results in Table 1 that the position of the maximum in the Y and Z direction seem to change from a pinhole to another. This is in fact not the case, this result is simply due to the fact that since the laser is inclined with a 30 degree angle to the horizontal, Y and Z coordinates are related, which means that there is not only one maximum but in fact many couples of values of Y and Z lead to a maximum in signal intensity when adjusting one parameter at a time. For this reason, and because it corresponds to the result that we obtained earlier that the position of maximum intensity in the Z direction is at 3.95 mm+ sample thickness, we chose to work at the positions that were measured for the smallest pinhole in the following experiments.

Another important conclusion for these results is that, even for the smallest pinhole, the interval of 5% tolerance is larger than one division of the micrometer of the stage which are 20 µm for the X and Y stages, and 10 µm for the Z stage. That means that adjusting the stages positions by eye with a precision of one division of the micrometer of the stage is enough to achieve a good alignment of the setup and to perform consistent measurements.

2.5 Background quantification

Because the goal of this project is to detect very low concentration of dye, we needed to make sure that that background noise is as low as possible. The first step in that direction was to quantify the background noise and to determine the influence of different parameters on the noise level. The first experiment we performed was done with the setup that is shown in Figure 5. Using this setup, we roughly aligned the laser in order to have a maximum in signal when targeting a piece of black tape positioned on the Z stage. We then performed measurements of the background noise with the laser on, with the laser off and we also made measurements of the background noise with an external source of light by turning on a desk lamp and targeting it away from the setup, the rest of the lab being in the dark. We then insulated the setup using pieces of tube and black tape, covering every hole in order to suppress the stray light as much as possible. A picture of the setup after insulation is shown in Figure 8.

In order to efficiently perform those measurements for different values of the PMT control voltage, we developed a LabView program to automatically control the DC power supply and the DAQ, as well as performing calculations of the mean value and standard deviation of the acquired data. This program is further described in appendix A of this report.

The background data obtained with the "open" setup and with the "insulated" setup are compared in figure 9. The data points correspond to the mean value of the output voltage of the PMT that was recorded for 1 s for each value of the control voltage, with a sampling rate of 10 kHz. We used a pinhole of 800 µm diameter and no ND filter was added in front of the laser. These result show that insulating the setup helped greatly diminishing the noise produced by external sources of light, the noise mean value with the desk lamp switch on in the lab being the highest for the open setup and dropping to the same level as the dark background noise when working with an isolated setup. Also, we can see that the dark background mean value of the isolated setup is significantly lower than that of the open setup. This is certainly caused by the fact that even if the light is switched off, the open setup still catches some stray

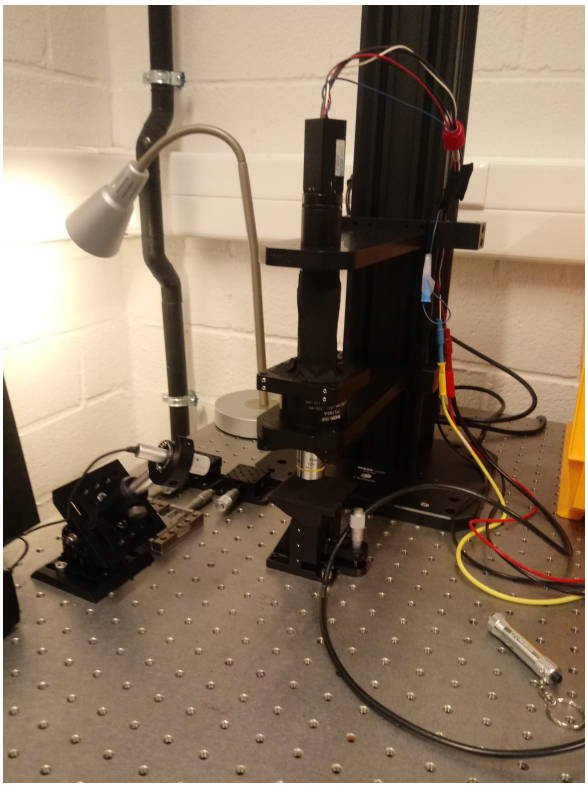

Figure 8: Picture of the "insulated" setup that was used to quantify the influence of external sources of stray ligh on the background noise level.

light from the instruments present in the lab and from the computer monitor, and insulating the setup suppresses this source of noise. For that reason, all the following measurements were performed with an isolated setup.

Another conclusion that we can draw from Figure 9 is that the noise produced by the laser is remarkably high. This is unexpected since the light from the laser should be blocked by the emission filter, its transmittance being lower than 10^{-8} at 635 nm, the peak wavelength of the laser, according to the manufacturer's specification sheet. The cause of this high value of the background noise due to the laser could be that the laser emits light with a wavelength that is transmitted by the emission filter. To verify this hypothesis, we measured the emission spectrum of the laser and we indeed observed a small peak of emission at longer wavelength. The explanation for the high noise value would then be that the light emitted by the laser was scattered by the black tape on the Z stage, then transmitted by the emission filter and finally detected by the PMT.

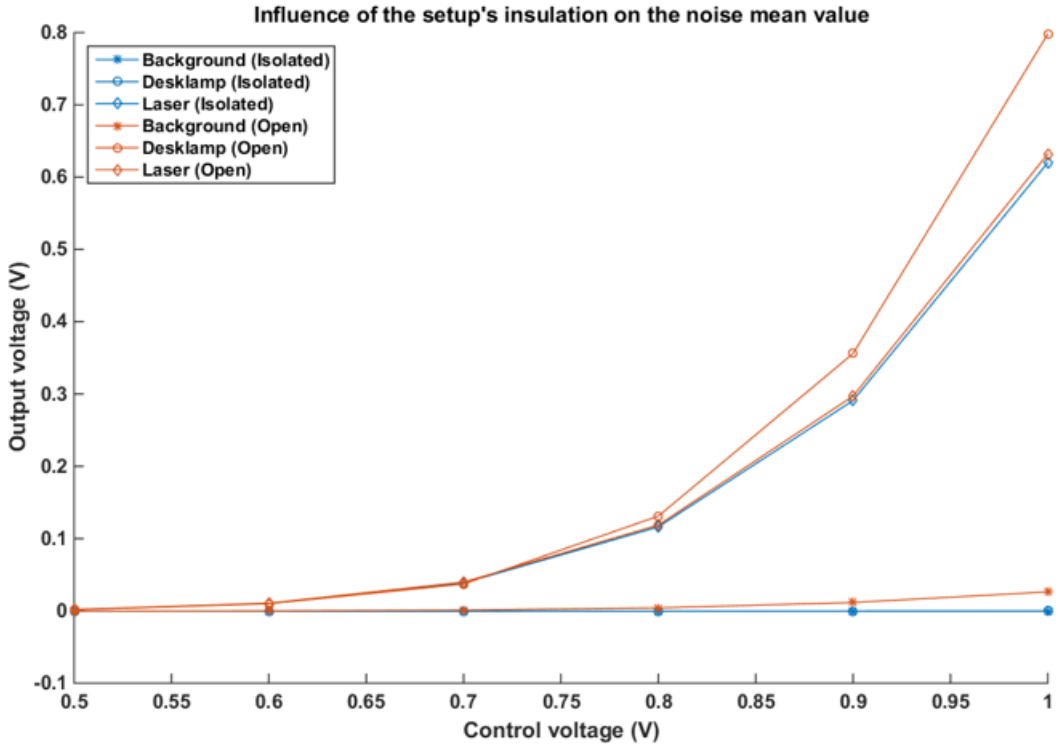

Figure 9: Background noise as a function of the control voltage before and after insulating the setup against stray light. The data labeled "Background" is the result of measurements done with every light switch off in the lab and the laser turned off. The "Desk lamp" data is the result of measurements done with a lamp switch on in the lab and the laser off. The "Laser" data results from measurements done with only the laser switched on.

To suppress this source of noise, we added the excitation filter in front of the laser to make sure that the light of longer wavelength emitted by the laser is blocked and doesn't reach the sample. This way, no light coming directly from the excitation source is detected by the PMT but only the longer wavelength light resulting from fluorescence.

We then made measurements of the background mean value for each pinhole, with and without excitation filter in order to determine its influence on the noise due to the laser. The measurements were performed with the same method as the previous background noise measurements, this time using each different pinhole. The data resulting from these measurements are presented in Figures 10, 11, 12 and 13 for pinhole diameters of 100, 200, 400 and 800 µm. These results show that the addition of an excitation filter to the setup significantly lowers the noise mean value when the laser is switched on, which confirms the hypothesis that the high value of the noise was due to the PMT detecting light emitted by the laser that was scattered by the black tape.

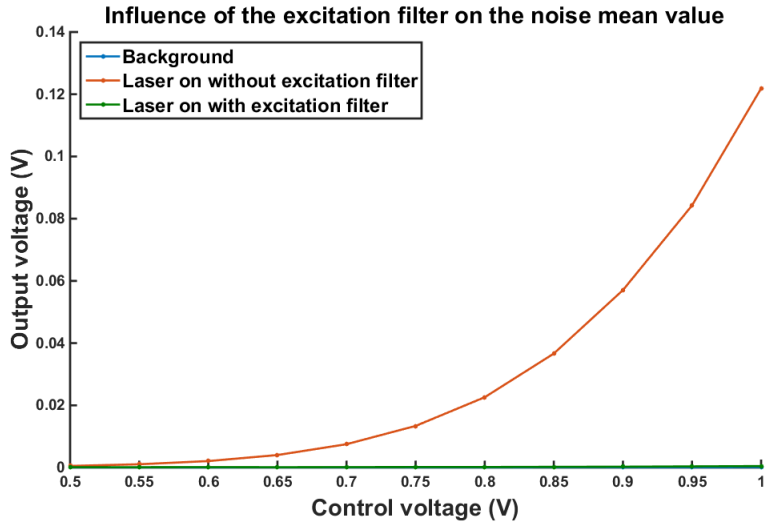

Figure 10: Comparison of the noise mean value with and without excitation filter using a 100 µm pinhole

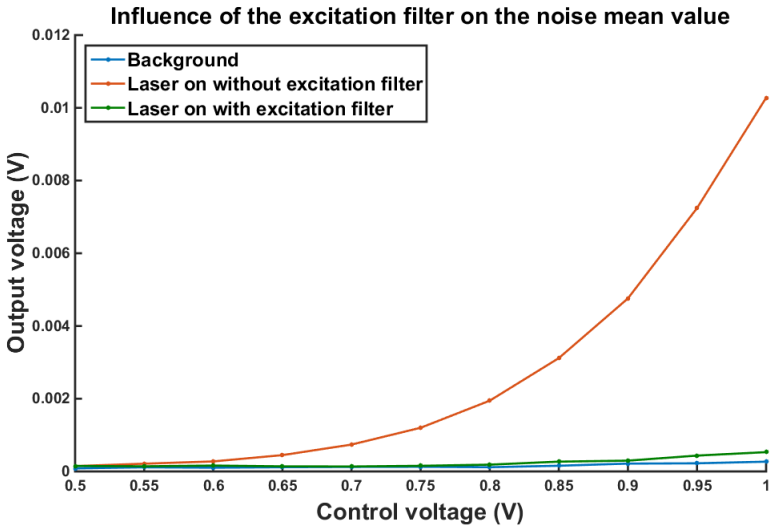

Figure 11: Comparison of the noise mean value with and without excitation filter using a 200 µm pinhole

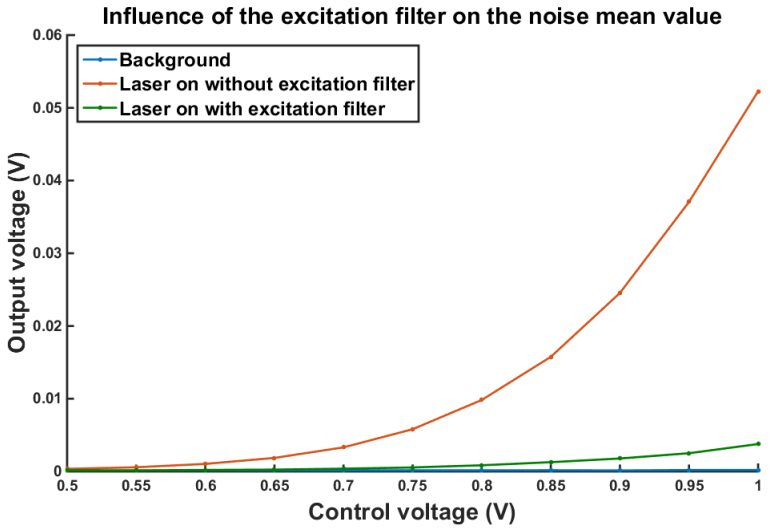

Figure 12: Comparison of the noise mean value with and without excitation filter using a 400 µm pinhole

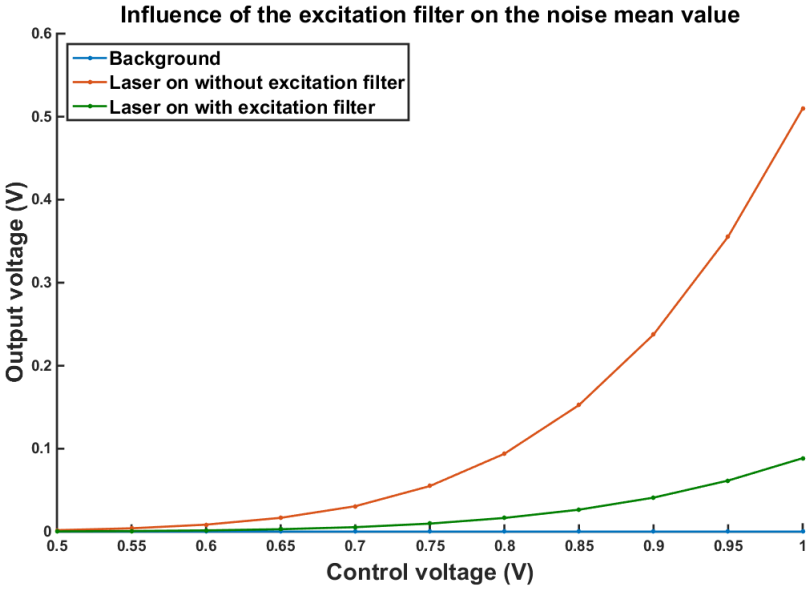

Figure 13: Comparison of the noise mean value with and without excitation filter using a 800 µm pinhole

Then, from the data previously acquired we calculated the ratio of the noise mean value to the background mean value for each pinhole, at 1 V control voltage. The results of those calculations are summarized in Table 2. these results show that the lowest ratio is obtained using the 200 µm diameter pinhole. Based on this criterion, we concluded that it the best pinhole diameter to use in the following measurements in order to have the lowest possible noise, and therefore to be able to detect the fluorescence signal from lower dye concentrations.

pinhole diameter (µm)	Noise to background ratio
100	3.9
200	2.0
400	19.2
600	18.1
800	412.0

Table 2: Noise to background ratios calculated for each pinhole from the mean value of the output voltage of the PMT.

3 Setup Calibration

Once the setup had been built and aligned, the next step was to make some measurements using a fluorescent target from Thorlabs in order to characterize and calibrate the output signal of the PMT for different parameters of pinhole diameter and laser power. For each pinhole diameter and ND filter, 1 s recordings of the output voltage were performed, at a sampling rate of 10 kHz using the LabView program. For each set of parameters, the measurements were done on 6 different spots of the sample and the final results were obtained by taking the average of the resulting data.

The plots of the output voltage as a function of the transmittance of the ND filter for each pinhole diameter and for a control voltage of 0.5 V is shown in Figure 14. As we can see from those results, the relationship between the output voltage of the PMT and the transmittance of the ND filter is almost linear. The reason for this is that the output voltage of the PMT is directly proportional to the fluorescence intensity, which is given by the product of the fluorescence quantum yield and the amount of light that is absorbed [2] :

$$F = \phi(I_0 - I) \tag{3}$$

where F is the fluorescence intensity, I_0 is the incident intensity, I is the transmitted intensity and ϕ is the fluorescence quantum yield, defined as the ratio of the number of photons emitted to the number absorbed.

Equation (3) can then be rewritten as follows using the Beer-Lambert law to express I as a function of I_0 :

$$F = \phi I_0(1 - 10^{-\epsilon lc}) \tag{4}$$

where ϵ is the molar extinction coefficient, l is the optical path length, and c is the concentration.

As we can see in equation (4), the relationship between the fluorescence intensity and the illumination intensity should be linear, and therefore, the relationship between the output voltage of the PMT and the laser intensity should be linear for a given control voltage and pinhole size.

To verify that, linear regressions were performed on the data for each pinhole diameter, the fits are represented in figures 15, 16 and 17 for pinhole diameters of 100, 400 and 800 µm. All results show a strong linear correlation, with linear correlation coefficients (r) above 0.99 for the two larger pinholes, and a slightly weaker linear correlation for the smaller pinhole with a coefficient of approximately 0.98.

One explanation to this slightly weaker linear correlation for the 100 µm diameter pinhole could be that since the pinhole is smaller, the fluorescence intensity that gets to the PMT comes from a smaller area of the sample, and therefore, the measurements could be impacted more by the sample non-uniformity.

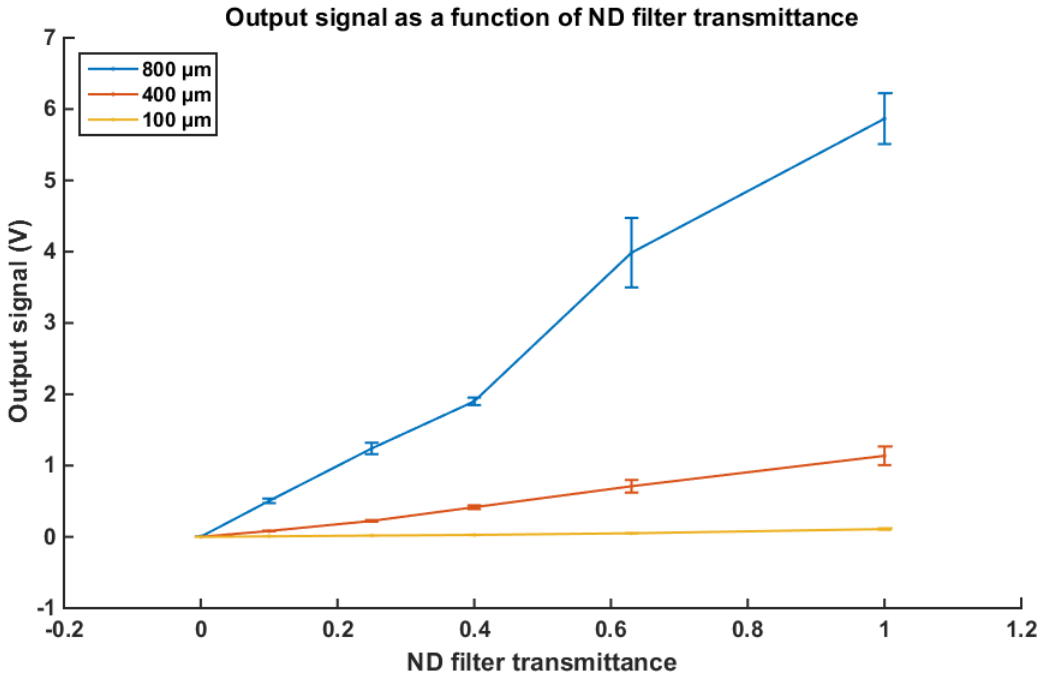

Figure 14: Output voltage of the PMT as a function of the transmittance of the ND filter placed in front of the laser (a transmittance of 1 corresponds to the laser without ND filter). The control voltage was set to 0.5 VThe data points were calculated by averaging over 6 spots of the sample. Error bars length corresponds to 2 standard deviations

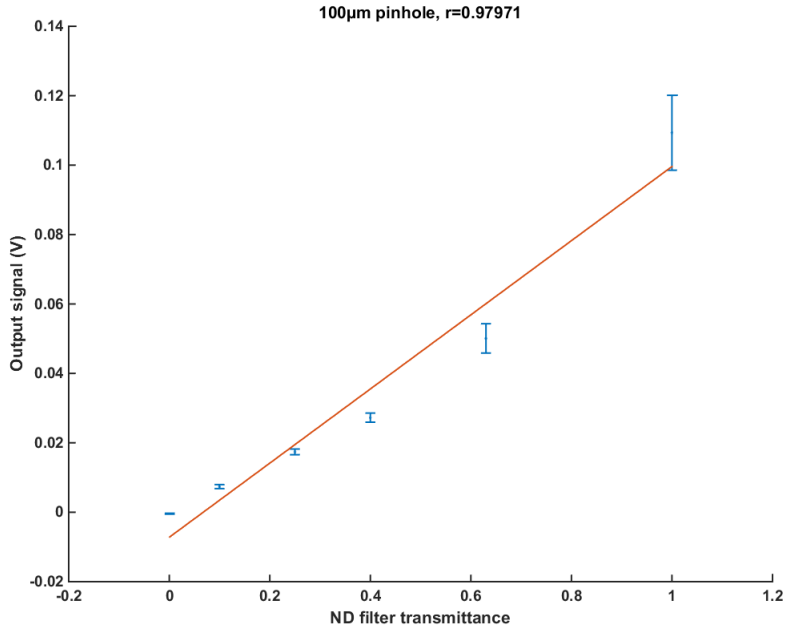

Figure 15: Linear fit of the data points of the output voltage of the PMT for different ND filters, with a 100 µm diameter pinhole. Fit of type y=ax+b with parameters a=0.1068 and b=-0.0072

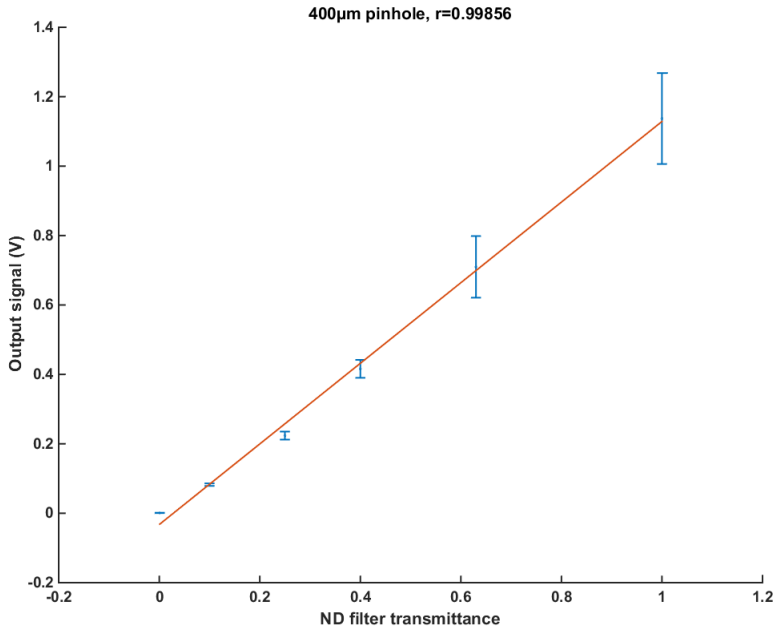

Figure 16: Linear fit of the data points of the output voltage of the PMT for different ND filters, with a 400 µm diameter pinhole. Fit of type y=ax+b with parameters a=1.16138 and b=-0.0326

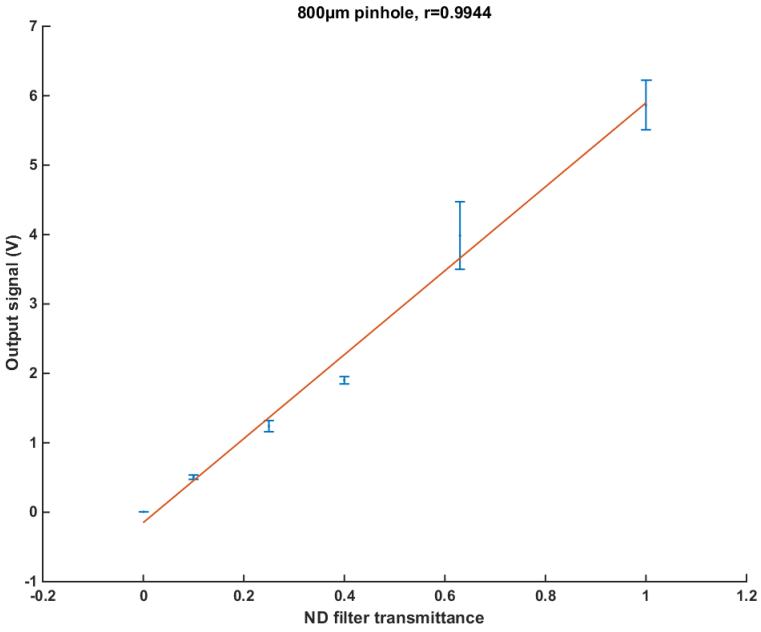

Figure 17: Linear fit of the data points of the output voltage of the PMT for different ND filters, with a 800 µm diameter pinhole. Fit of type y=ax+b with parameters a=6.0468 and b=-0.1491

The results for the calibration of the output voltage of the PMT as a function of the pinhole diameter using different ND filters are shown in Figure 18. Those measurements were performed using a control voltage of 0.55 V. Because the intensity of the light getting through the pinhole is obviously proportional to the surface area of the aperture, one would expect the output voltage to be proportional to the pinhole diameter squared.

This is confirmed by the fittings shown in figures 19 to 24, in which the data points were fitted with a curve of equation $y = ax^2 + b$. For each ND filter that was used, we can see that the data were fitted really well by the model, with an R^2 value above 0.99 for each fit.

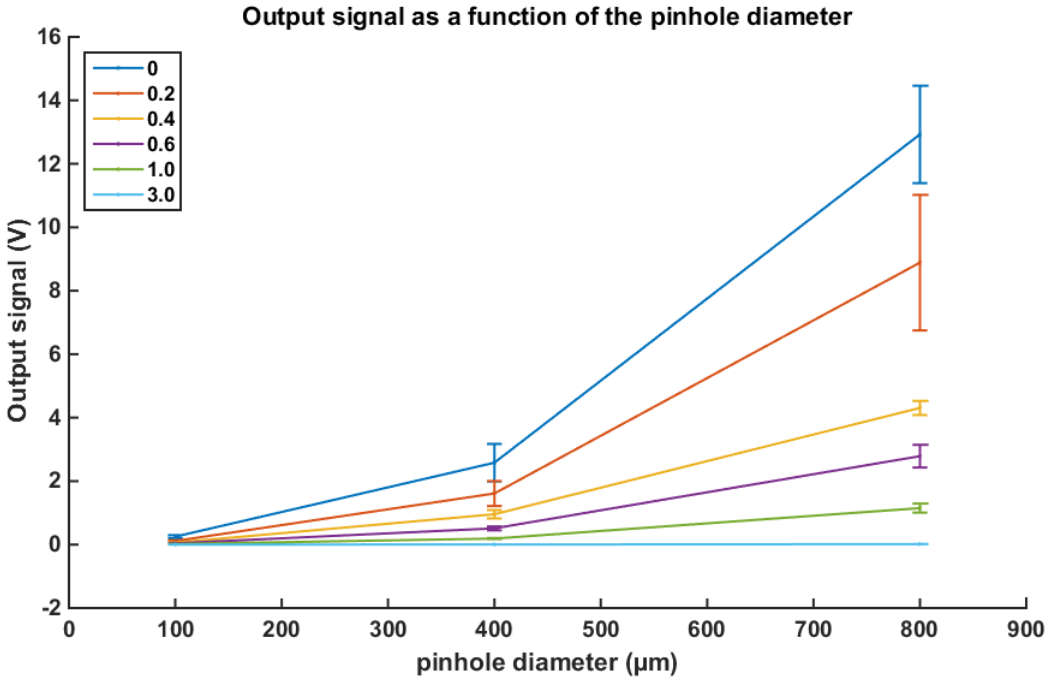

Figure 18: Output voltage of the PMT as a function of the diameter of the pinhole. The control voltage was set to 0.55 VThe data points were calculated by averaging over 6 spots of the sample. Error bars length corresponds to 2 standard deviations

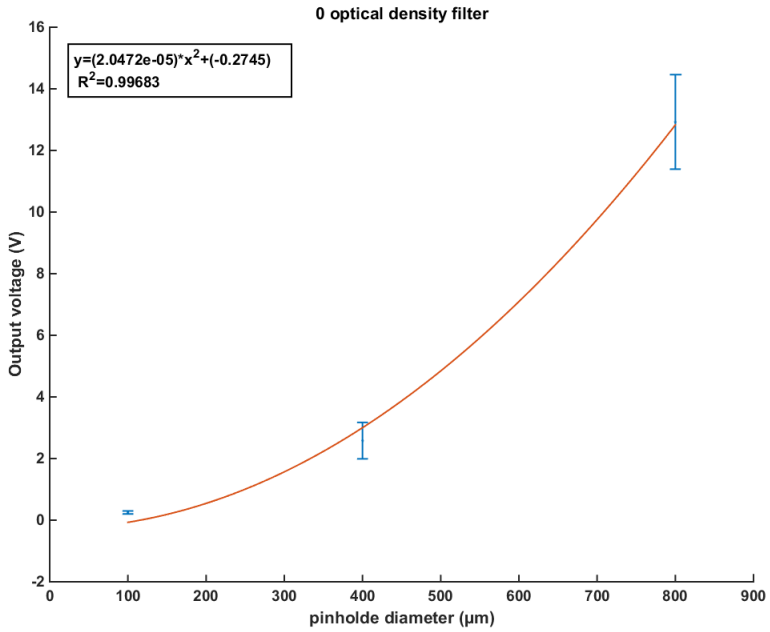

Figure 19: Fit of the data points of the output voltage of the PMT for different pinhole diameters, using the laser without ND filter

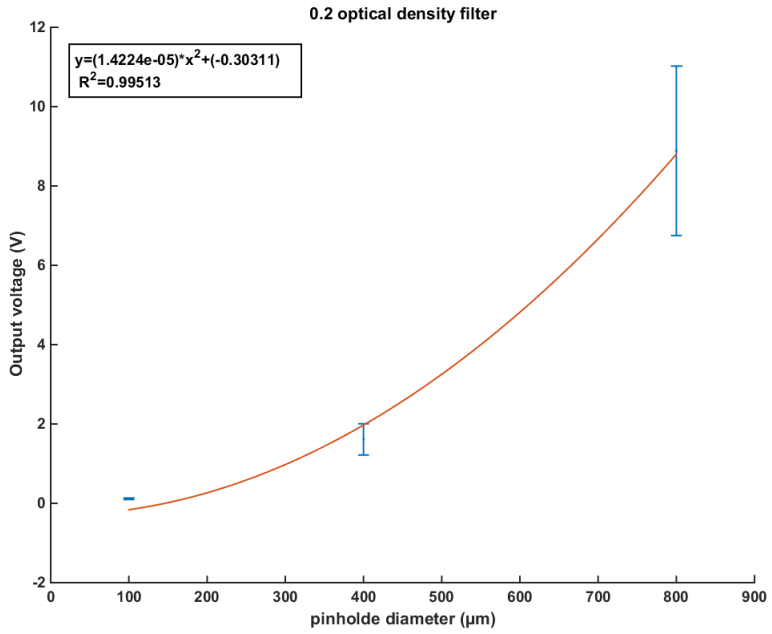

Figure 20: Fit of the data points of the output voltage of the PMT for different pinhole diameters, using a ND filter of 0.2 optical density.

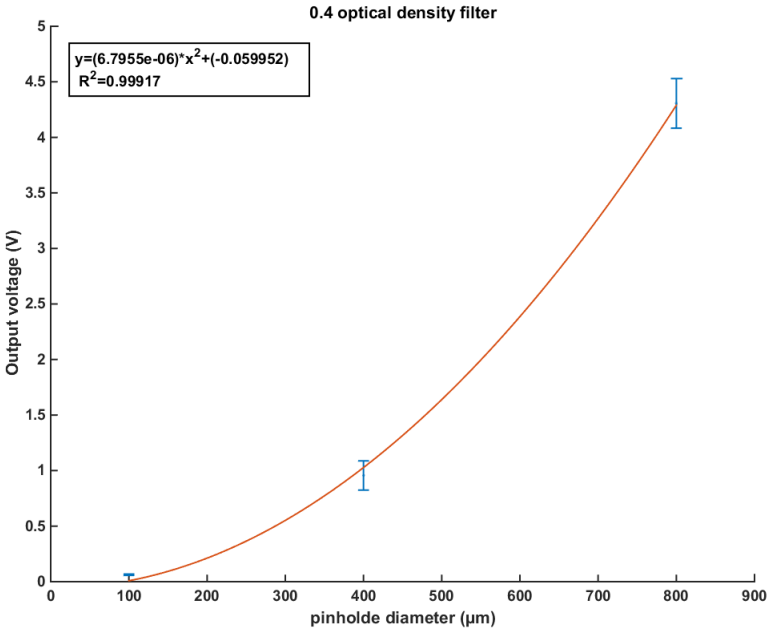

Figure 21: Fit of the data points of the output voltage of the PMT for different pinhole diameters, using a ND filter of 0.4 optical density.

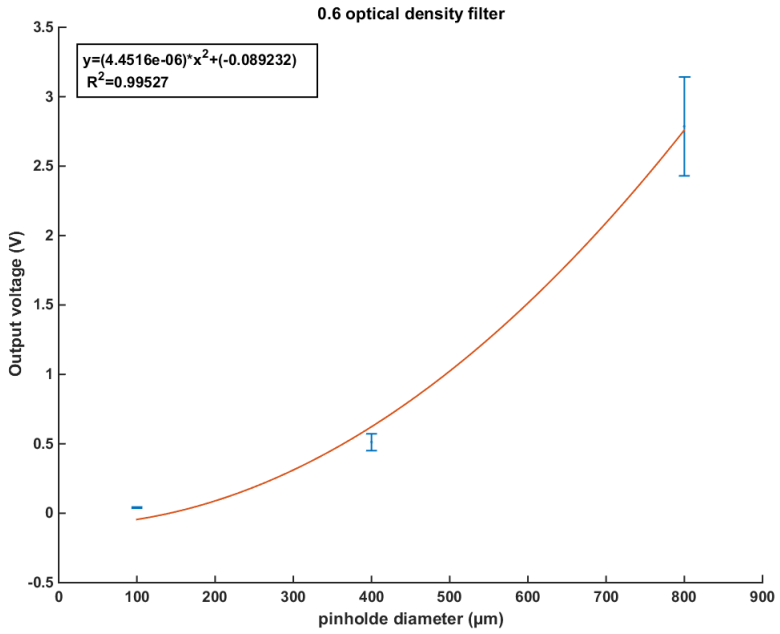

Figure 22: Fit of the data points of the output voltage of the PMT for different pinhole diameters, using a ND filter of 0.2 optical density.

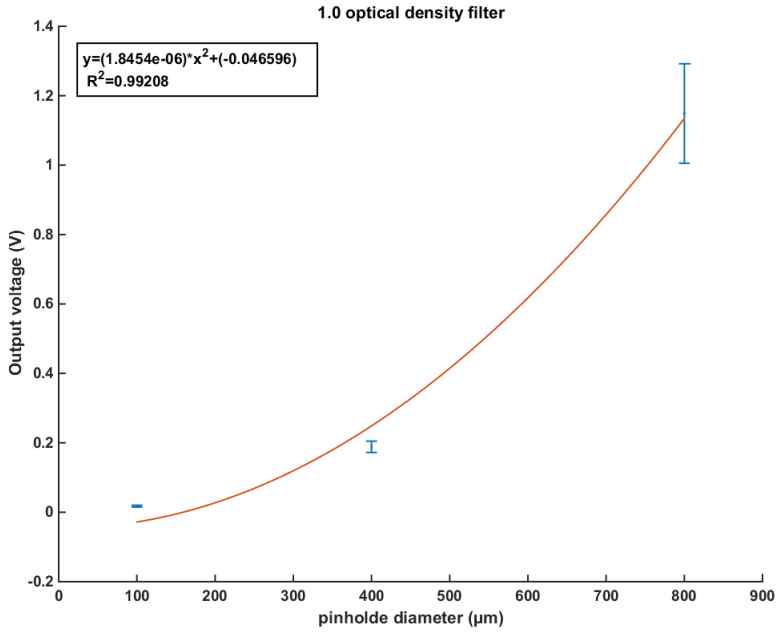

Figure 23: Fit of the data points of the output voltage of the PMT for different pinhole diameters, using a ND filter of 0.2 optical density.

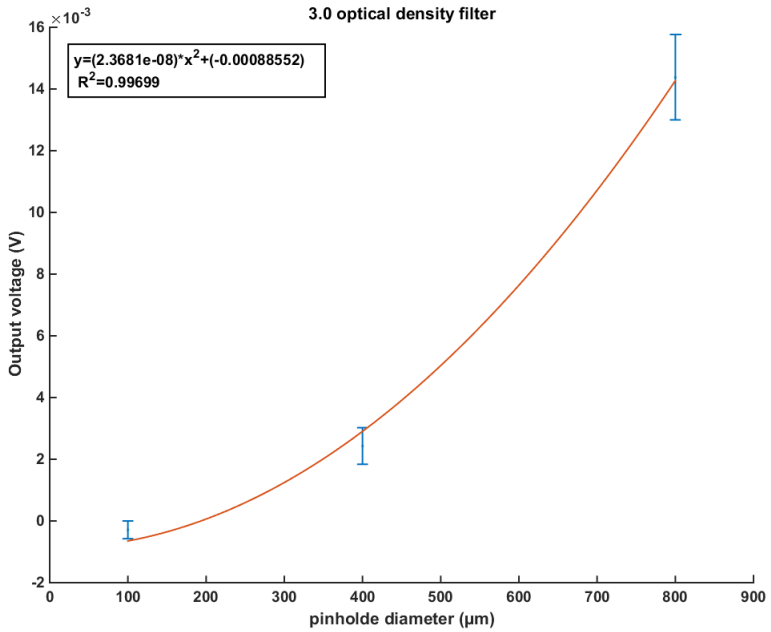

Figure 24: Fit of the data points of the output voltage of the PMT for different pinhole diameters, using a ND filter of 0.2 optical density.

4 Sample preparation

The samples that were used in the limit of detection and photobleaching measurements were prepared following the protocol that we describe in this section.

The dye we used was Alexa Fluor 647, as we mentionned earlier in this report. Several solutions of different concentrations were already available in the lab and were stored in the fridge, protected form the light. The different solutions were labeled No. 1 to 7, from higher to lower concentration, as described in Table 3. For easier reading, we will from now on refer to these solutions using their label.

Label	Concentration
No. 1	$1\,\mathrm{mg\,mL^{-1}}$
No. 2	$0.1\,\mathrm{mg\,mL^{-1}}$
No. 3	$0.01\,\mathrm{mg\,mL^{-1}}$
No. 4	$1\,\mathrm{\mu g\,mL^{-1}}$
No. 5	$0.1\,\mathrm{\mu g\,mL^{-1}}$
No. 6	$0.01\,\mathrm{\mu g\,mL^{-1}}$
No. 7	$1\,\mathrm{ng\,mL^{-1}}$

Table 3: Alexa Fluor 647 solutions labeling by concentration

To prepare the samples, droplets of known volume of dye solution were placed on support slides using a micro-pipette. The slides were then kept in a dark environment until completely dry. In order to be able to compare the different samples, we needed to quantify the amount of dye molecules that are being illuminated by the laser when performing the fluorescence measurements. The concentration of the solution cannot be used directly as a comparison criteria because the amount of dye molecules that are illuminated by the laser also depends on the surface area of the dried droplet. For this reason, we used the following formula (equation (5)) to assign a surface density to the samples.

$$\rho_A = \frac{CV}{\pi r^2} \tag{5}$$

where ρ_A is the average surface density, C is the concentration of the dye solution V is the volume of the droplet, and r is the approximate radius of the dried droplet.

To use this formula, we need to make the assumption that the dried droplet is uniform and disc-shaped, which is a rough approximation. In fact, we determined that the samples systematically gave more fluorescence signal towards the edges of the dried droplet, which means that the samples are not uniform. To compensate for this non-uniformity, all the measurements were performed with the laser approximately targeting the center of the sample.

5 Determination of the limit of detection

The main goal of this project is to determine the lowest possible dye concentration that can be detected by our setup, and with what set of parameters. That means we need to determine the limit of detection of the setup. The limit of detection is based on the signal-to-noise ratio (SNR) of the measurements, which is defined as follows [3]:

$$SNR = \frac{\mu_{Signal} - \mu_{Background}}{\sigma_{\mathbf{Noise}ackground}} \tag{6}$$

where μ_{Signal} is the mean value of the signal and $\mu_{Background}$ and $\sigma_{Background}$ are the mean value and the standard deviation of the background noise respectively.

There are different ways to define the limit of detection, but we will use the most common one which is to define it at SNR=3. This means that only measurements with a SNR above this limit are meaningful and any measurement with a SNR below 3 is considered inconclusive.

This section includes the results of our measurements of the SNR for different dye concentrations and different settings of the setup.

5.1 Influence of the support slide on the background

To calculate the SNR, we first needed to quantify the background noise. Because the sample is deposited on a support slide, we have to take into account the influence of the slide on the background noise, so we started by measuring the signal from blank slides. There were three types of slides available in the lab that could be used as a support for our samples : 1mm thick polyamide microscope slides (PA), 1 mm thick superamide microscope slides (SA) and 0.13-0.16 mm thick cover glass slides. Just by placing the slides on the stage, we could easily see by eye that the light from the laser was scattered in a really different manner by the different types of slides. In order to determine the best slide to use, we quantified the background noise from all three types of slide.

The first step was to measure the signal from the blank slides as a function of the position of the stage in the Z direction. The result of one of those measurements is shown in Figure 25 for a cover glass slide. We can see two peaks in this plotting, at Z=3.78 and at Z=3.9, which could be due to light scattering on the upper and lower surface of the cover slide since those peaks are separated by a distance approximately equal to the thickness of the slide. The same measurements were performed on the PA and SA slides and we measured a maximum at Z=4.45 for the PA slide and at Z=4.65 for the SA slide. Those measurements were done with the 800 µm diameter pinhole in order to maximize the output voltage. For the same reason, a control voltage of 1 V and no ND filter were used.

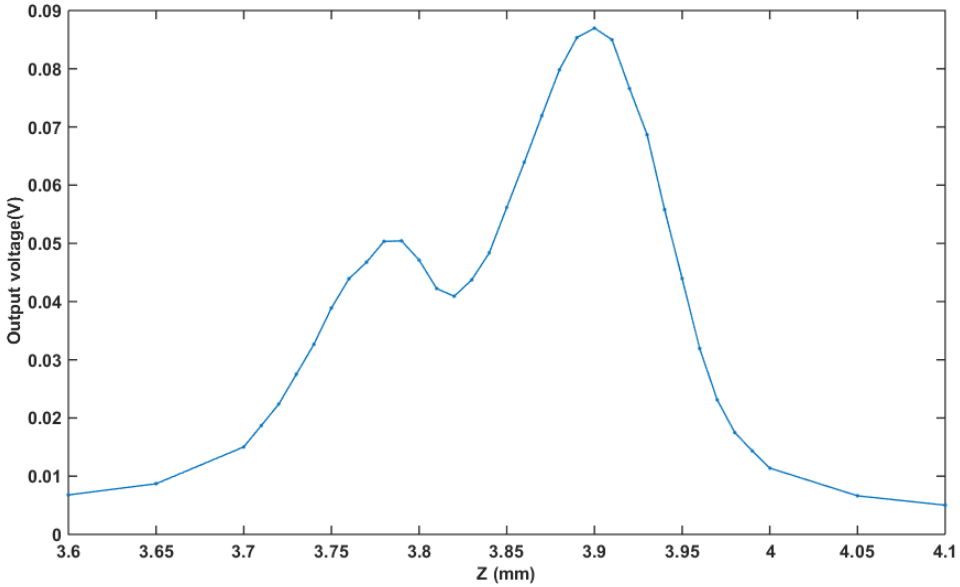

Figure 25: Output voltage of the PMT as a function of the position of the stage in the Z direction when illuminating a blank cover glass slide. In order to have enough signal, a 800 µm diameter pinhole, a control voltage of 1 V and no ND filter were used .

To compare the background noise from the different slides, we measured the signal from the blank slides on 6 different spots, using the 200 µm diameter pinhole, a control voltage of 1 V and no ND filter. The measurement were 1 s recordings at a sample rate of 10 000 Hz, made using the LabView program that we developed. The Z stage was placed to the position of the maximum for each type of slide (Z=3.90 for the cover glass slide, Z=4.45 for the PA slide and Z=4.65 for the SA slide). Because the cover glass slides showed some impurities, we also made those measurements on a cover glass slide that was cleaned with ethanol, to determine whether cleaning it would lower the background level.

The results of these measurements are shown in Figure 26. As we can see from this figure, the lowest background noise level is obtained using the PA microscope slide, with $0.634 \pm 1.532\text{mV}(mean \pm SD)$ at maximum PMT gain. We also can see that cleaning the cover slide lowered significantly the background noise from this type of slide. We can conclude from these results that the best slide to use in order to have a high SNR would be the PA slide since it produces a noise that has approximately half the mean value and half the standard deviation of the noise produced by the SA slide.

Unfortunately, there was not enough stock of PA and SA slides in the lab at the time of the measurements so we had to work with the cover glass slides for the upcoming measurements, which is not optimal.

5.2 SNR measurements

To calculate the SNR, we first had to make measurements of the background noise from blank cover glass slide for each parameter of laser power and PMT gain, following the same protocol as for the previous background measurements, averaging over 6 different spots on the slide for each different settings. These measurements of the background noise were then used to calculate the SNR that are presented in the following sections.

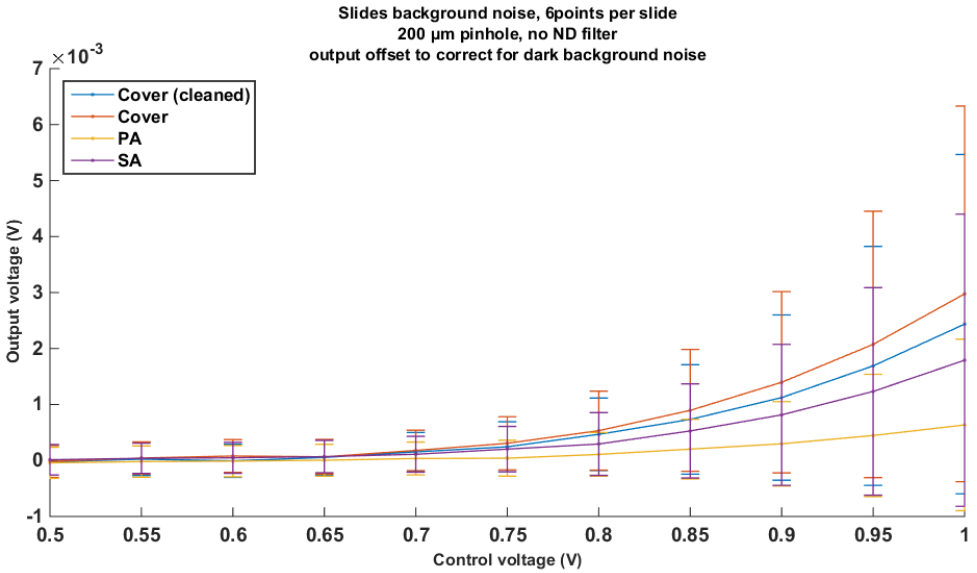

Figure 26: Background noise of blank slides as a function of the control voltage of the PMT. The dark background noise was deduced from the data. Bars represent two standard deviations.

5.2.1 Influence of the laser power

To determine the influence of the laser power on the SNR, we prepared one sample of each solution from No.3 to No.7. We did not take time to prepare samples using the first two solutions because we had no doubt that they would give a lot of signal and therefore a high SNR. The samples were prepared following the protocol that we described earlier, using a volume of 1 µL of solution for each sample. The samples were then put on the Z stage so as the laser approximately targets the center of the droplet. For each sample, we recorded the output voltage of the PMT for 1 s with a sampling rate of 25 kHz using DAQ Express. We did so for each laser power by changing the ND filter in front of the laser between each measurement. All the measurements were done with a PMT control voltage of 1 V.

In order to protect the sample from photobleaching, the laser was turned off between each measurement and we modified the laser power from the lowest to the highest, starting with the ND filter of 2.0 optical density and ending with no ND filter for each different sample.

The mean value of the signal was then computed and, alongside with the background data, was used to calculate the SNR of the measurements, using the formula from equation (6). The results are shown in Figures 27 to 31.

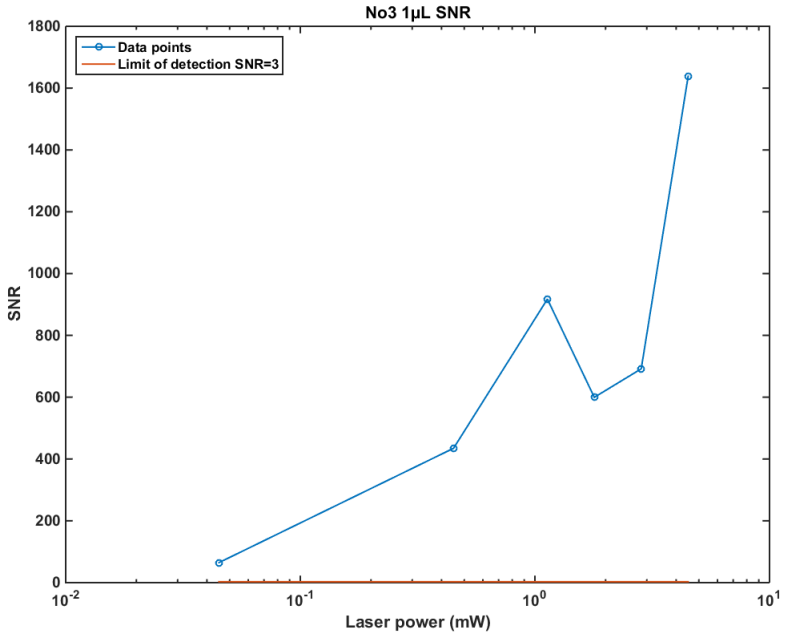

Figure 27: SNR as a function of the laser power. Calculated from measurements on a 1 µL sample of solution No.3

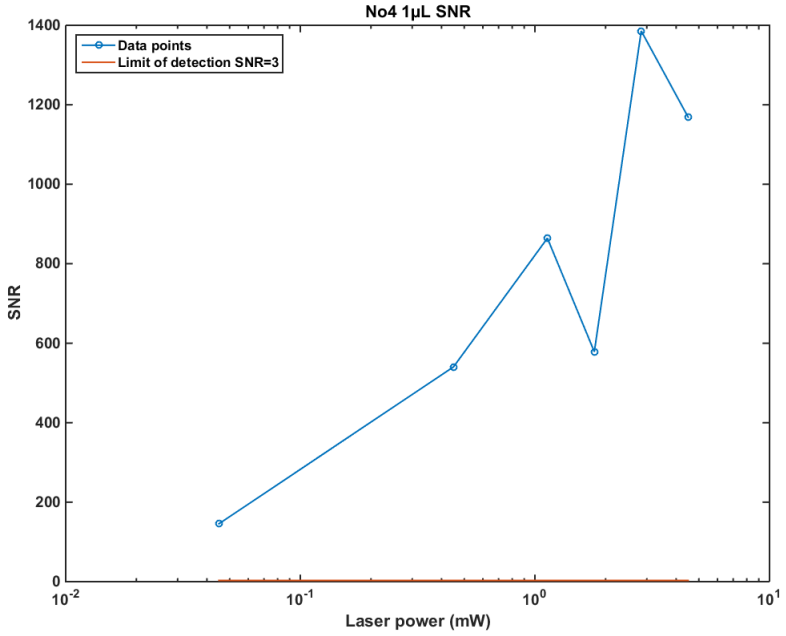

Figure 28: SNR as a function of the laser power. Calculated from measurements on a 1 µL sample of solution No.4

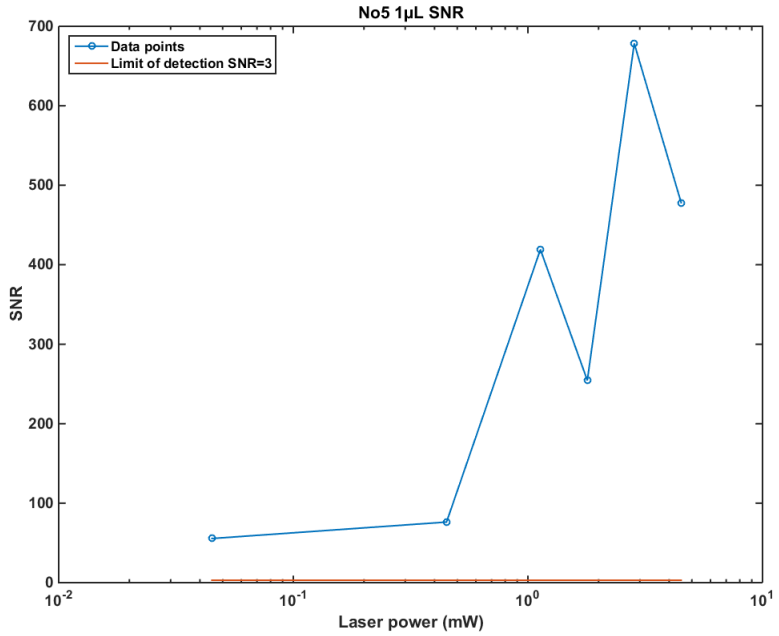

Figure 29: SNR as a function of the laser power. Calculated from measurements on a 1 µL sample of solution No.5

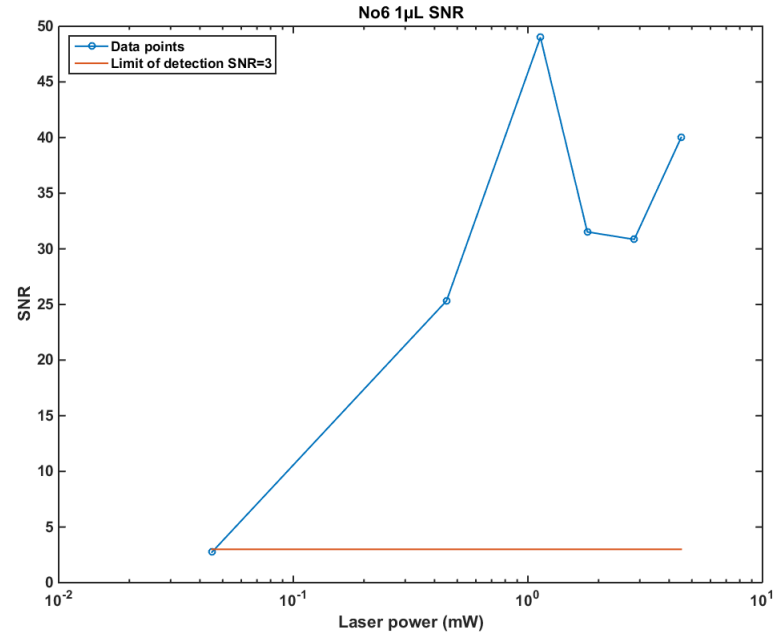

Figure 30: SNR as a function of the laser power. Calculated from measurements on a 1 µL sample of solution No.6

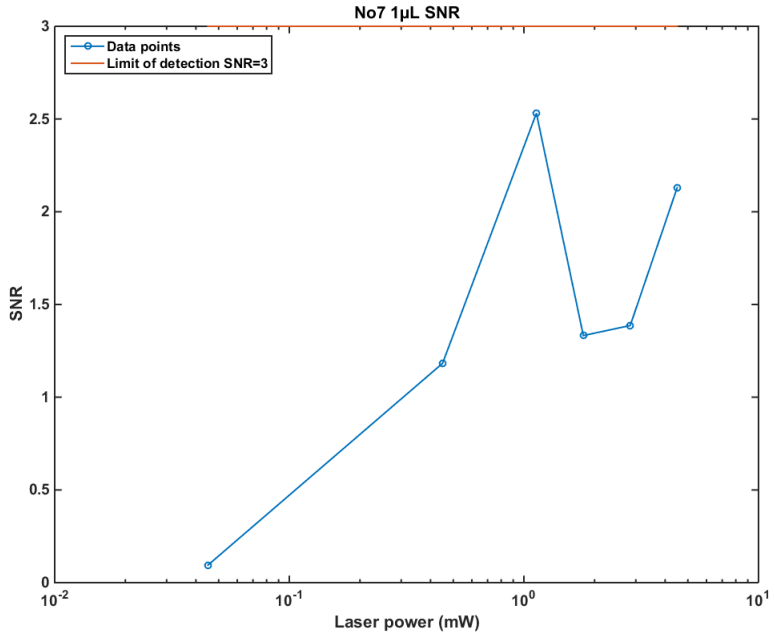

Figure 31: SNR as a function of the laser power. Calculated from measurements on a 1 µL sample of solution No.7

We can see from those results that the samples made from solutions No.3 to No.5 give enough signal to have a SNR way above the limit of detection, even for the lowest laser power which is 0.045 mW and corresponds to the addition of a 2.0 optical density filter in front of the laser. This is not the case for the sample prepared from solution No.6 for which the measurement at 0.045 mW has a SNR below 3, an is therefore below the limit of detection (see Figure 30). The results from Figure 31 show that all measurements done on the sample made from solution No.7 have a SNR below the limit of detection, which could mean that the current setup is unable to detect such low concentration of dye.

However, we can also see that the curves produced by our results have an unexpected shape. In fact one would expect the SNR to increase with increasing laser power. This is globally the case but all the results show a maximum at 1.13 mW laser power, which corresponds to the addition of a 0.6 optical density filter in front of the laser, then the SNR drops and starts increasing again when we increase the laser power.

The first explanation to this unexpected behaviour is that the drop of SNR is caused by photobleaching. Because the same sample was used for all the measurements varying the laser power, it had already been illuminated for some time when the measurements at higher laser power were performed. The dye in the sample could have been altered due to this exposure to light through the process of photobleaching, leading to a fluorescence signal increasing slowlier than the background noise when the laser power increases and therefore leading to a drop in SNR.

To test this hypothesis, a second set of measurement was conducted, this time using a new sample each time the laser power was modified. No other parameter or setup setting was changed. For this experiment we focused on solution No.6 and No.7 since we can easily see from the previous results that the higher concentrations are above the limit of detection of the setup, even for a low laser power. The results from this set of measurements are shown in Figures 32 and 33.

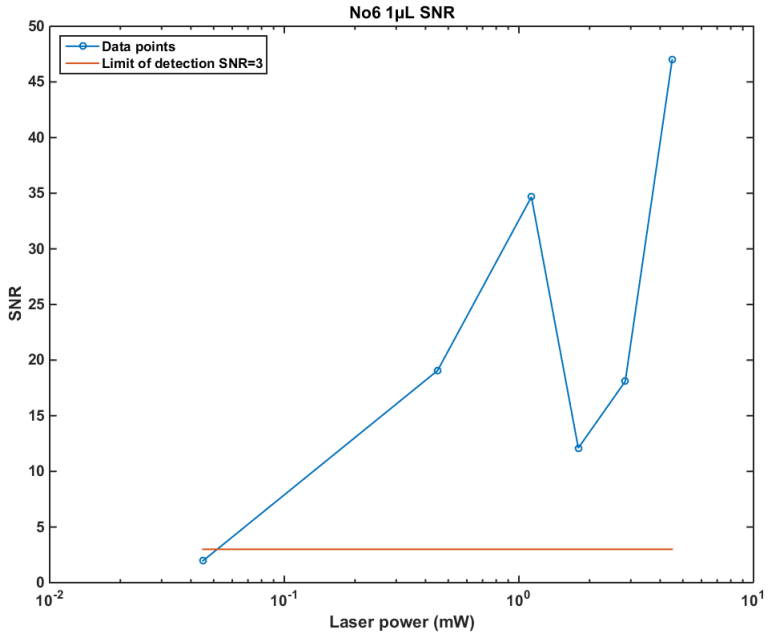

Figure 32: SNR as a function of the laser power. Calculated from measurements on 1 µL samples of solution No.6, using a new sample for each measurement.

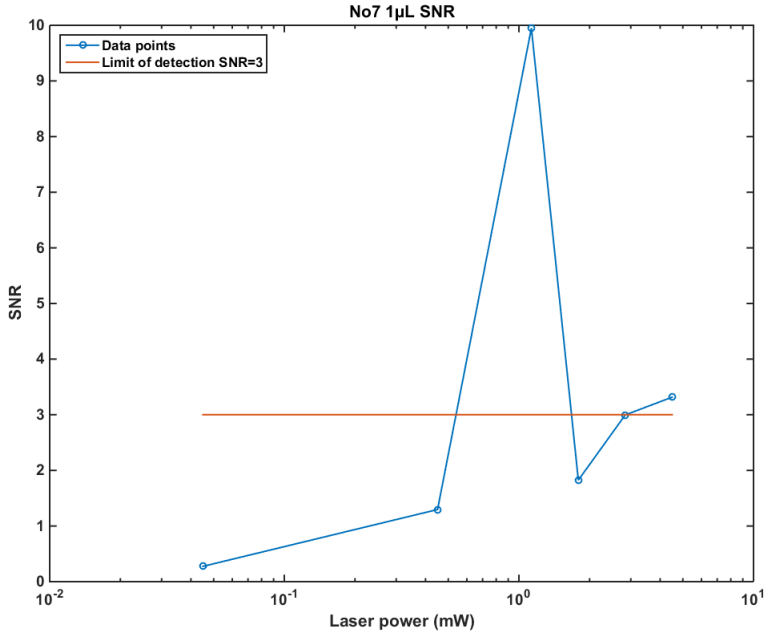

Figure 33: SNR as a function of the laser power. Calculated from measurements on 1 µL samples of solution No.7, using a new sample for each measurement.

As we can see in Figures 32 and 33, the peak at 1.13 mW remains, even though this time it cannot be caused by photobleaching since the samples were new for each measurements. On the other hand photobleaching could still be a important limiting factor, especially at low dye concentration, since we can see that the maximum SNR reached for solution No.7 in the previous set of measurements was approximately 2.5 (see Figure 31) whereas using a new sample for each measurement allowed to reach a SNR of about 10 (see Figure 33).

To determine the cause of the peak in SNR at 1.13 mW laser power, we can look separately at the mean value of the fluorescence signal and the mean value and standard deviation of the background noise. This data is represented in Figures 34, 35 and 36 for the measurements performed on solution No.7 samples.

Looking at this data, we can clearly see where the peak in SNR comes from since the output voltage of the PMT also features a peak for 1.13 mW laser power and the decreases going from 1.13 to 1.79 mW whereas the background mean value and standard deviation keeps increasing. This peak in output signal is in disagreement with the results that we got previouslyduring the calibration of the setup that showed that the output voltage of the PMT is linearly related to the laser power. However, this peak could not be caused by a random experimental error such as the non uniformity of the sample because it is featured in all of our results.

One plausible explanation for this phenomenon is that the introduction of a ND filter in front of the laser slightly modifies the lateral position of its waist, which means that some ND filters could focus the laser on the sample in a better way than others. In this case, that would mean that the 0.6 optical density filter, which corresponds to a laser power of 1.13 mW, focuses the laser on the sample but the 0.4 optical density filter, which corresponds to a laser power of 1.79 mW focuses the laser either before or past the sample, leading to a wider and less intense spot of illumination on the sample and therefore to a lower fluorescence intensity.

Because of the limited duration of the internship, this hypothesis was not tested and further experiments would be needed to verify it. For example, the laser focus could be adjusted upon changing ND filters in order to guarantee that it is focused on the surface of the slide.

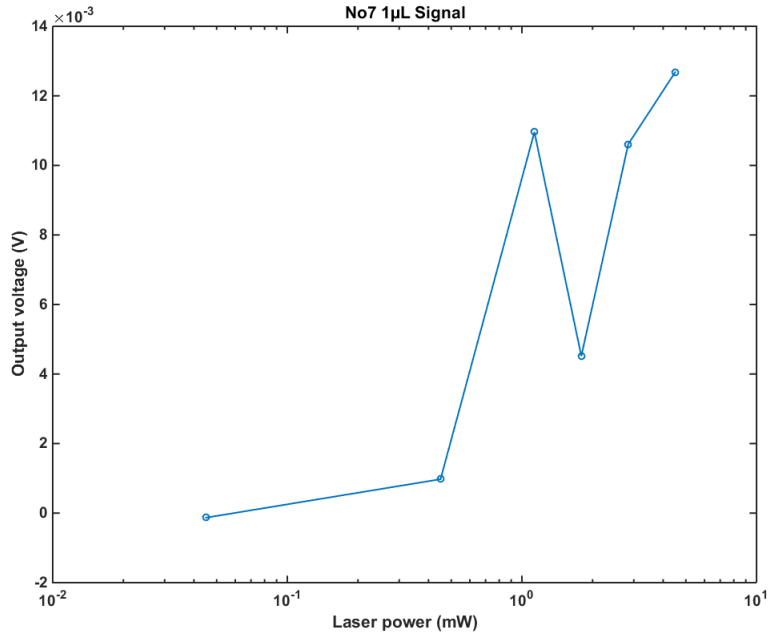

Figure 34: Mean value of the fluorescence signal as a function of the laser power. Calculated from measurements on 1 µL samples of solution No.7, using a new sample for each measurement.

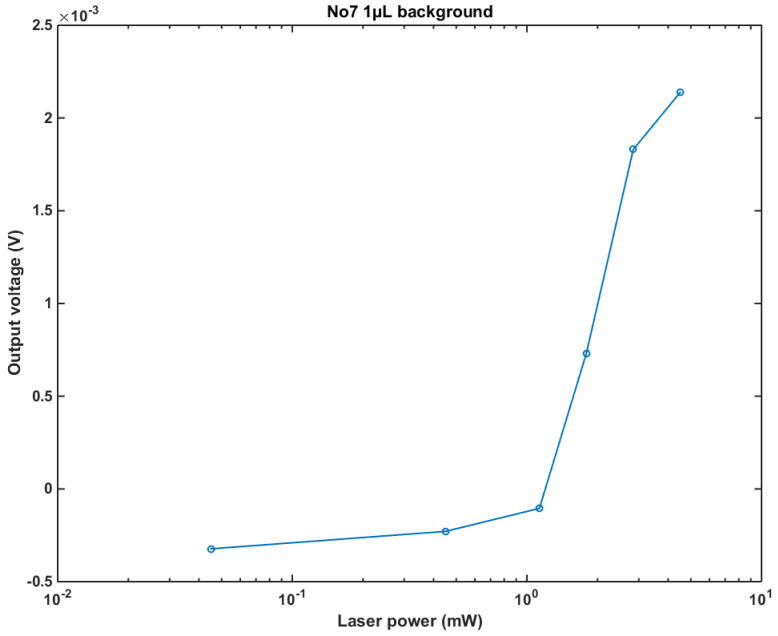

Figure 35: Background mean value as a function of laser power. Calculated from measurements on a blank cover glass slide, averaging over 6 spots of the slide

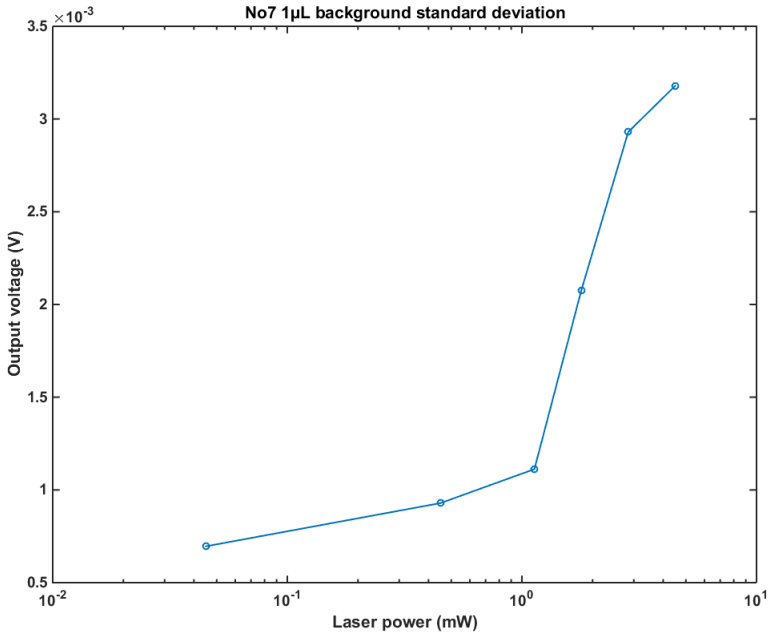

Figure 36: Background standard deviation as a function of laser power. Calculated from measurements on a blank cover glass slide, averaging over 6 spots of the slide

5.2.2 Influence of the PMT gain

The second parameter whose we wanted to determine the influence on the SNR was the gain of the PMT. In the previous measurements, we assumed that the highest gain would lead to the highest SNR and we set the control voltage of the PMT to 1 V for each measurement. But because increasing the gain of the PMT not only amplifies the fluorescence signal but also amplifies the background noise and its oscillations, we needed to perform measurements with different control voltages in order to verify our hypothesis.

For this experiment, the laser power was set to it's maximum, which is 4.5 mW, by adding no ND filter. The output voltage of the PMT was recorded for 1 s at a sampling rate of 25 kHz. The samples were 1 µL samples of solutions No.6 and No.7, prepared following the protocol described in section 4. Measurements were done for three values of the control voltage : 0.5 V, 0.75 V and 1 V and a new sample was used for each value of the control voltage. As for the previous measurements, we used the 200 µm diameter pinhole.

From these measurements, the SNR was calculated using the formula from equation (6) and using the background data from blak cover glass slides that was previously acquired. The results are shown in Figures 37 and 38 for samples made from solutions No.6 and No.7, respectively. These results confirm that a higher PMT gain implies a higher SNR, which confirms our hypothesis.

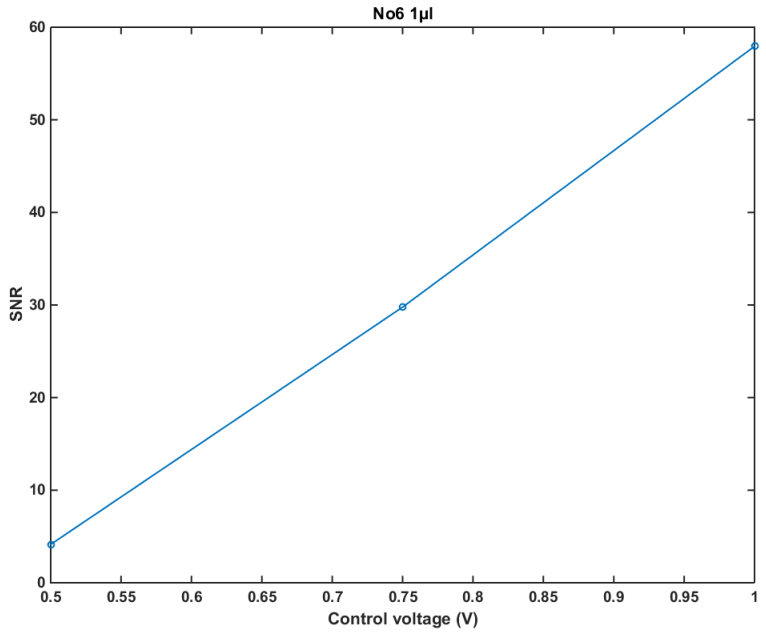

Figure 37: SNR as a function of the control voltage of the PMT. Calculated from measurements on 1 µL samples of solution No.6, using a new sample for each measurement.

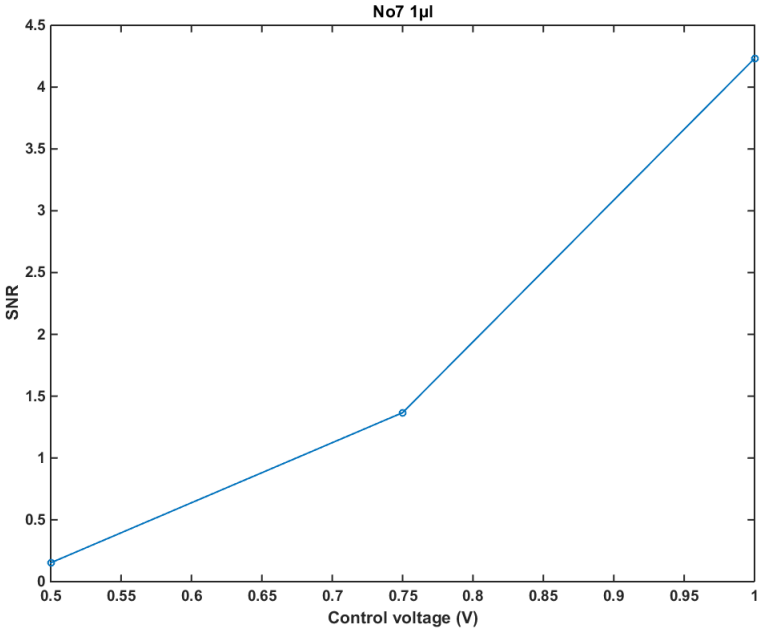

Figure 38: SNR as a function of the control voltage of the PMT. Calculated from measurements on 1 µL samples of solution No.7, using a new sample for each measurement.

5.3 Conclusions and perspectives

To conclude this section, we determined that our setup could detect a fluorescence signal from samples made from dye solutions as little concentrated as $1\,\mathrm{ng\,mL^{-1}}$ (solution No.7). This limit of detection depends on the power of the laser and on the gain of the PMT, a lower limit of detection being achieved by increasing the power of the illumination and the gain of the PMT.

We also determined that this limit of detection could easily be improved in two ways. The first one would be to use PA microscope slides instead of cover glass slides. Such a modification could significantly increase the SNR since we measured that the background noise mean value and standard deviation for these slides are less than half the ones of the slides we used in our SNR measurements. On the other hand, the presence of a peak at 1.13 mW laser power in our measurements of the SNR as a function of the laser power could indicate that the laser focus was not optimally adjusted during our measurements, especially for the lower optical density filters. As a consequence, the SNR could also be increased by adjusting the laser focus, and therefore, an even lower limit of detection could be achieved.

6 Photobleaching quantification

Photobleaching is the photochemical alteration of a fluorophore leading to a loss of it's ability to fluoresce. Photobleaching is a really important factor in the current experiment, as in every fluorescence-based measuring method because it leads to the removal of fluorophore molecules from the pool of active molecules in the target as the sample is excited by the light source. Less active molecules means less fluorescence signal and therefore the signal decreases over time as the sample is illuminated. The rate at which photobleaching occurs is specific to the fluorophore that is studied, but also depends on the excitation intensity and fluorophore concentration [4]. It is therefore important to quantify how fast the photobleaching occurs in our experiment for different laser power and concentration parameters in order to determine its impact on the results.

6.1 Methods

In order to quantify the photobleaching rate, $1\mu l$ samples of solutions No.6 and No.7 (see Table 3) were prepared on cover glass slides following the method described in section 4. The samples were then put under the microscope objective so as the laser illuminates approximately the center of the dried droplet. The output voltage of the PMT was recorded for 10 minutes at a sampling rate of 10 kHz, starting just before the introduction of the sample under the objective. The pinhole diameter was set to $200\mu m$ and the control voltage of the PMT was set to 1.0 V.

The data was then smoothed using a moving average filter with a window size of 1001 points, and fitted with a double exponential model using the following equation from Szabó et al. (1992) [5] :

$$Y = A + Be^{-X/T_1} + Ce^{-X/T_2} \tag{7}$$

6.2 Results and discussions

As we can see in the following figures (Figures 39 to 45), the bleaching data is well fitted by equation (7), and the photobleaching kinetics can be seen as the sum of a fast exponential decay and a slower one. In order to avoid any confusion, we will refer to the time constants of those two components as T_{fast} and T_{slow} from now on. Their values are summarized in table 4 for each experimental parameters that were studied.

The reason for this non-single exponential decay behavior is that several photochemical reactions are responsible for photobleaching, and each one of them occurs at its own rate and depends on different parameters. The reactions occuring in the specific case of Alexa Fluor 647 were not investigated as it would take a much more detailed study to describe them.

Solution	Optical density	T_{fast}	T_{slow}
No. 6	0.0	6.294247	114.057982
No. 6	0.4	17.402290	207.853383
No. 6	1.0	53.657290	733.144313
No. 6	2.0	34.749987	257.014658
No. 7	0.0	19.425304	189.954585
No. 7	0.4	23.290041	186.221612
No. 7	1.0	19.878533	208.276180

Table 4: Time constants of the components of the double-exponential fittings of the photobleaching data for each solution and each optical density filter studied.

However, supposing that the mechanisms in question are similar to those described in Song et al. (1995) [4] in their study of the kinetics of fluorescein, we can conduct the same analysis as they did to explain the double-exponential behaviour of the photobleaching kinetics of Alexa Fluor 647. Their analysis is that the photochemical reactions leading to photobleaching can be grouped in two main mechanisms which are the dye-to-dye mechanism (D-D) and the dye-to-oxygen mechanism (D-O), accounting respectively for the chemical reactions between dye molecules and between dye molecules and surrounding molecular oxygen. The D-D mechanism is strongly dependent on the concentration of fluorophore because the likelyhood for fluorophores to interact with eachother depends on the average intermolecular distance, therefore on the concentration. For the same reason, the D-O mechanism depends on the intermolecular distance between dye molecules and molecular oxygen. Because the sample is freely exposed to air during the measurement, the average intermolecular distance between dye molecules and oxygen molecules should be constant, whereas the average distance between dye molecules increases over time as the reaction goes on, leading to a decreasing probability for D-D reaction. That's why a switching-over is observed, where the photobleaching reaction is first dominated by the D-D mechanism until the distance between fluorophores gets too large for them to interact and the D-O mechanism starts to dominate the reaction.

If we apply this analysis to our results, we can conclude that the slow component of the double-exponential is due to reactions between dye molecules and oxygen molecules, and the fast decaying component is due to reactions between two dye molecules. Supposing this is the case, we should see an increase in both time constants as the concentration of the solution decreases This is the case when we look at the results without optical density filter for solutions No.6 and No.7 in table 4, but when we consider the other results, we can't see any obvious trend.

The relationship between the time constants and the laser power is not obvious either, looking at the results for solution No.6, the time constants seem to increase with decreasing laser power, except for the results for the 1.0 optical density filter, which look abnormal and could be the consequence of experimental errors or due to non-uniformity of the sample. On the other hand, the time constants look constant with respect to laser power when we look at the results for solution No.7 (Figures 43 to 45).

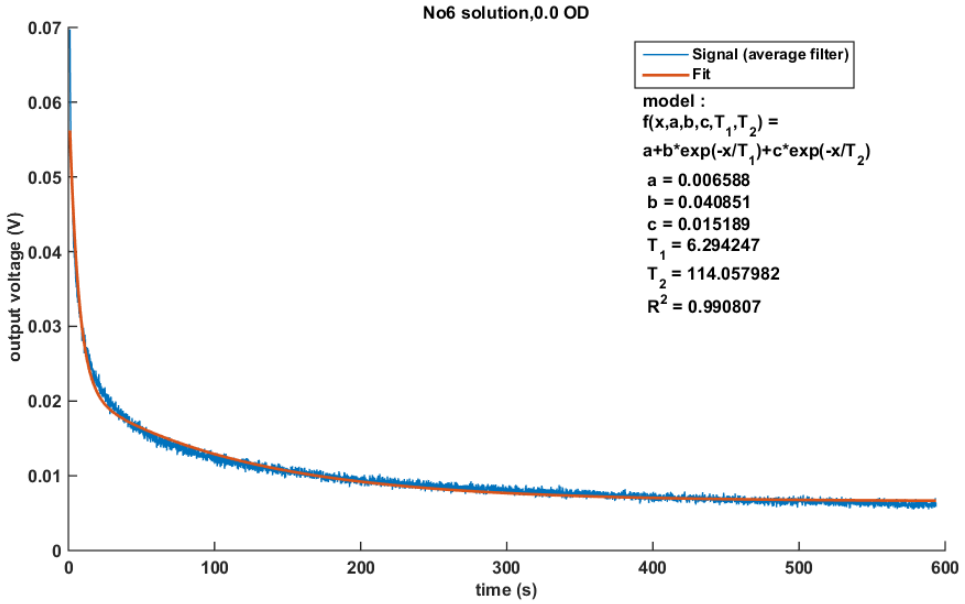

Figure 39: Double exponential fitting of the photobleaching data for a 1 µLl sample of solution No. 6, o was added in front of the laser.

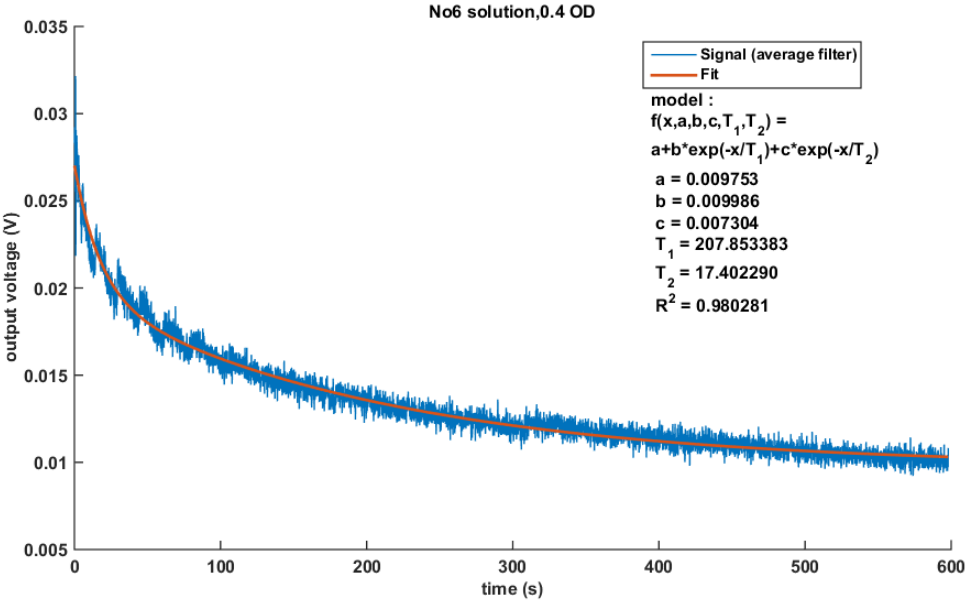

Figure 40: Double exponential fitting of the photobleaching data for a 1 µL sample of solution No. 7, using an ND filter of 0.4 optical density.

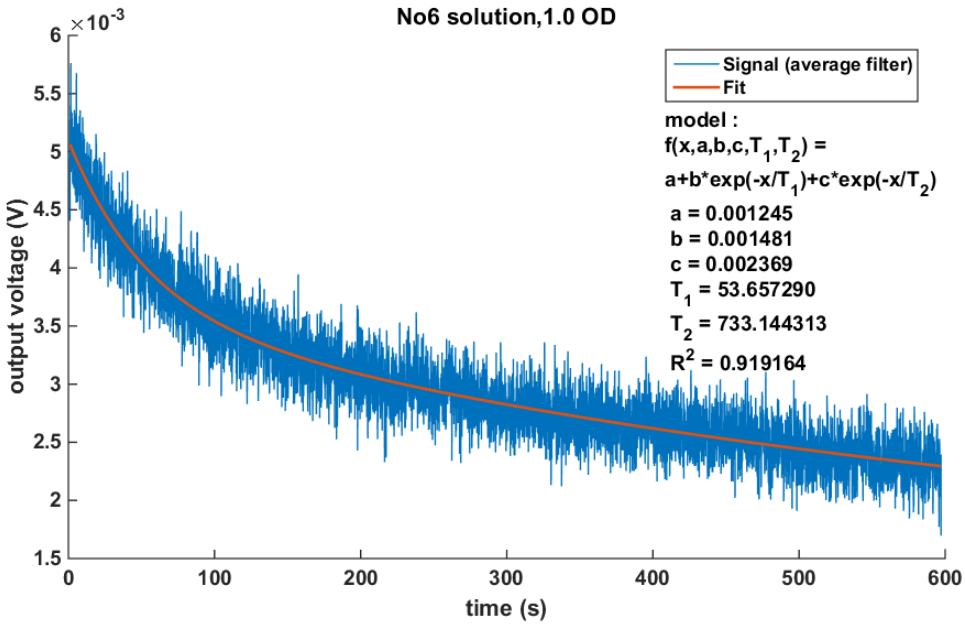

Figure 41: Double exponential fitting of the photobleaching data for a 1 µL sample of solution No. 6, using an ND filter of 1.0 optical density.

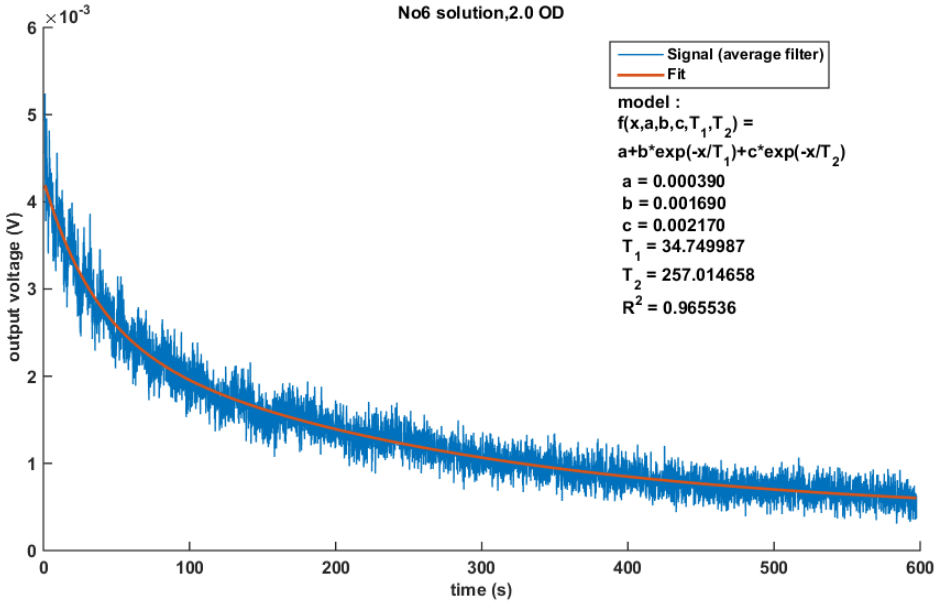

Figure 42: Double exponential fitting of the photobleaching data for a 1 µL sample of solution No. 6, using an ND filter of 2.0 optical density.

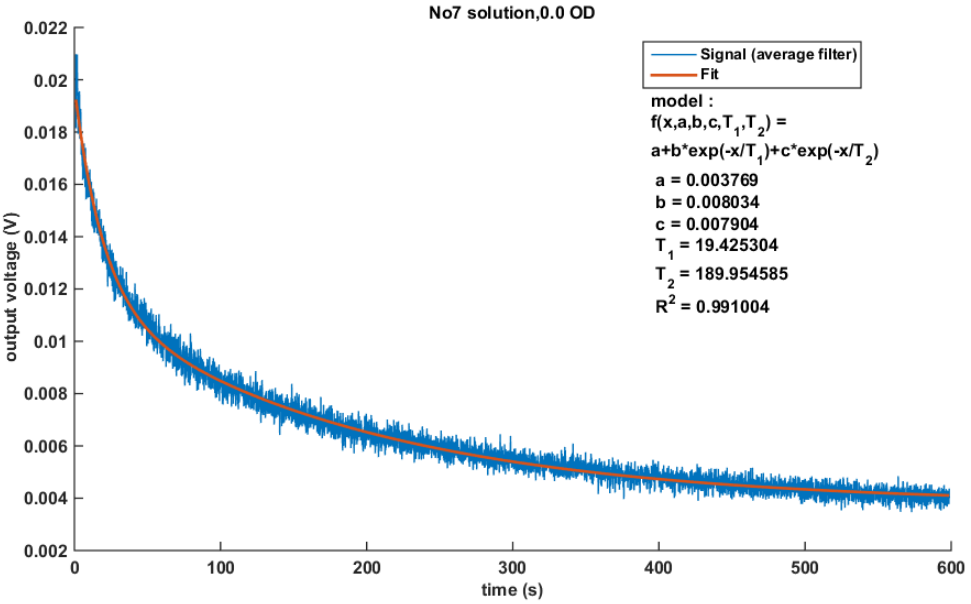

Figure 43: Double exponential fitting of the photobleaching data for a 1 µL sample of solution No. 7, no ND filter was added in front of the laser.

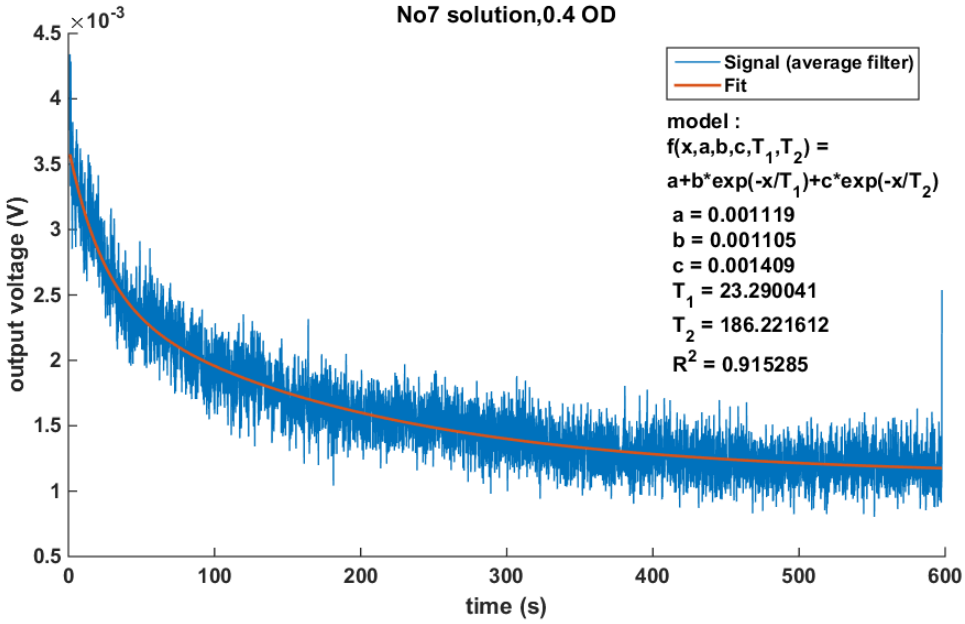

Figure 44: Double exponential fitting of the photobleaching data for a 1 µL sample of solution No. 7, using an ND filter of 0.4 optical density.

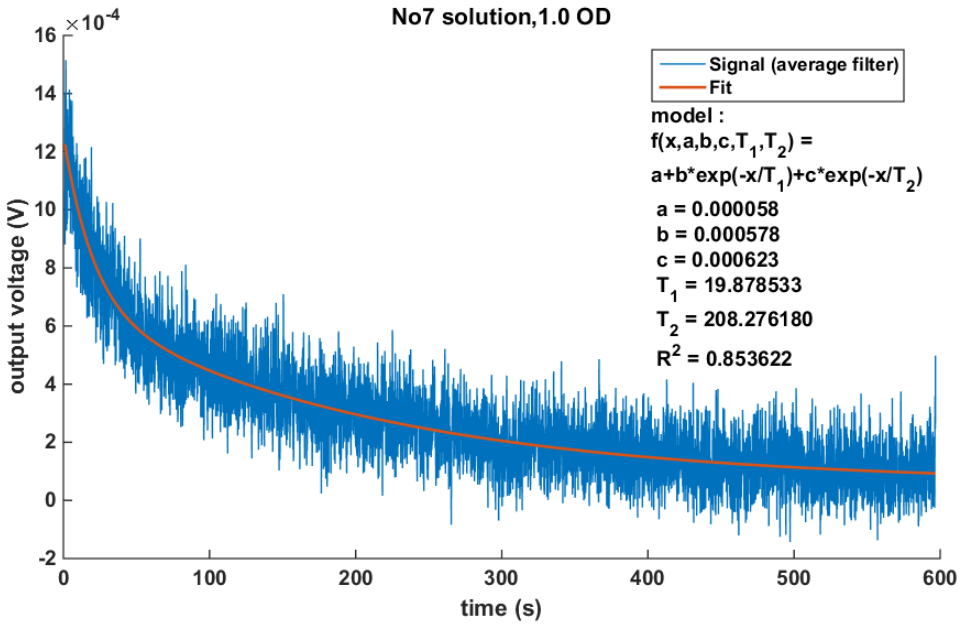

Figure 45: Double exponential fitting of the photobleaching data for a 1 µL sample of solution No. 7, using an ND filter of 1.0 optical density.

6.3 Comparison with previous results

In order to confirm the validity of the fitting model, we applied it to results that were obtained by Yunfeng Nie prior to this internship, with a similar setup. The samples that were used in those experiments were different in volume and in composition from the samples studied here, so no quantitative comparison can be done with our results. Despite those differences, we can see that the model we used also fits well the photobleaching data, as shown in figures 46 and 47, with an R^2 value over 0.95 for all three fittings.

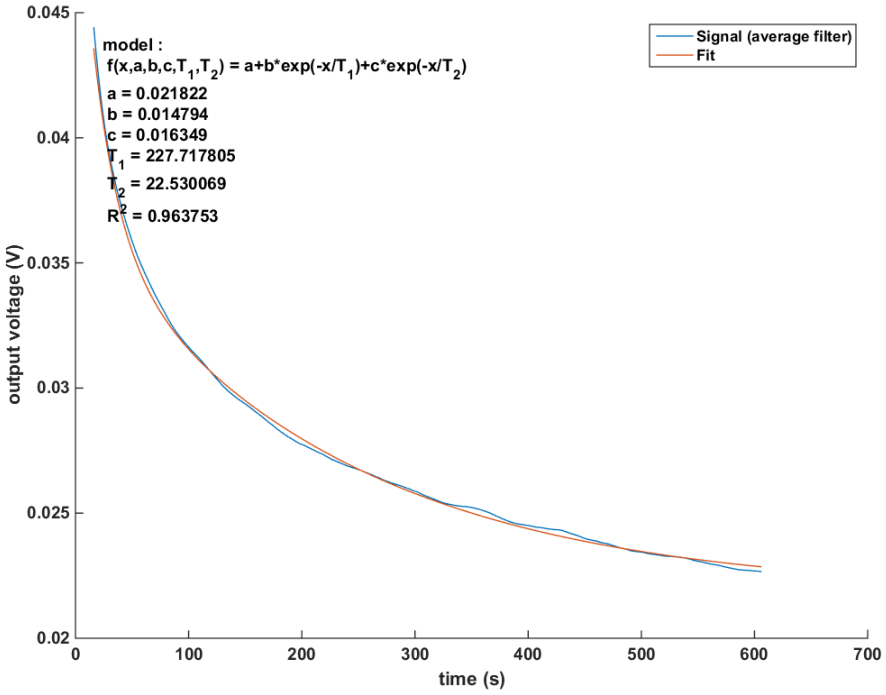

Figure 46: Double exponential fitting of the photobleaching data for a control voltage of 1V and using 2.0 ND filter.

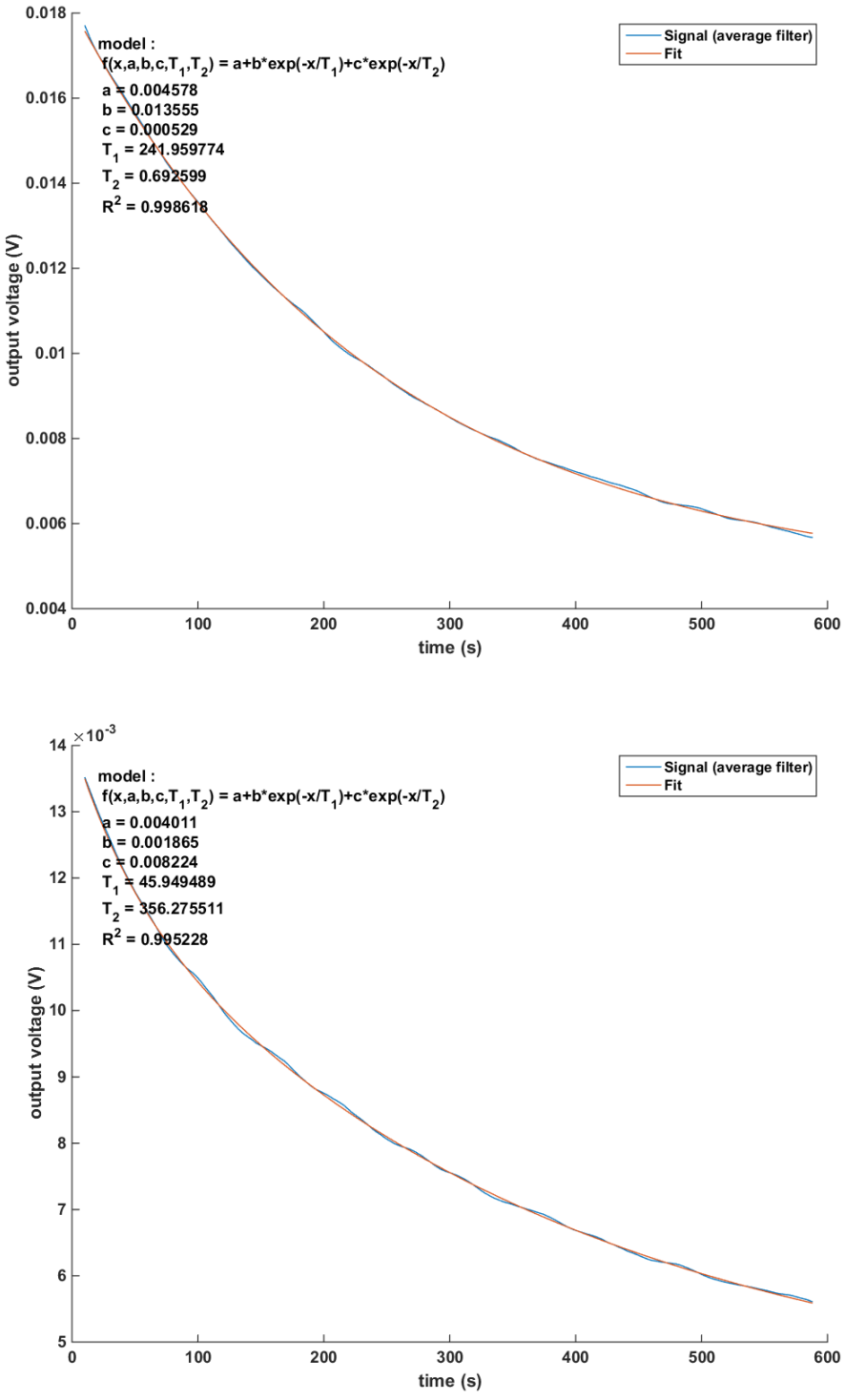

Figure 47: Double exponential fitting of the photobleaching data for a control voltage of 1V. The two plottings correspond to two different spots on the same sample.

6.4 conclusions and perspectives

As a conclusion for this section, we showed the validity of a double exponential model to fit photobleaching data in the case of our fluorescence detection setup. This tool could make a quantification of the photobleaching kinetics possible but the current results can't lead to solid conclusions and further experiments would be needed. A simple way to improve the results and unveil a meaningful relationshipbetween the photobleaching time constants, solution concentration and laser power would be to increase the number of measurements. This way the errors due to the sample non-uniformity could be compensated, as well as other experimental errors.

References

[1] Stefan Wilhelm. *Confocal laser scanning microscopy.* Carl Zeiss Microscopy GmbH, Carl-Zeiss-Promenade 10,07745 Jena,Germany.

[2] THEODORE K. CHRISTOPOULOS and ELEFTHERIOS P. DIAMANDIS. 14 - fluorescence immunoassays. In Eleftherios P. Diamandis and Theodore K. Christopoulos, editors, *Immunoassay*, pages 309 – 335. Academic Press, San Diego, 1996.

[3] Tom Verschoten. *Towards multi-measurement lab-on-a-chip systems.* PhD thesis, Vrije Universiteit Brussel, 8 2015.

[4] Li Yan Song, Everhardus Hennink, Ian Ted Young, and Hans Tanke. Photobleaching kinetics of fluorescein in quantitative fluorescence microscopy. *Biophysical journal*, 68 6:2588–600, 1995.

[5] G. Szabó, P.S. Pine, J.L. Weaver, M. Kasari, and A. Aszalos. Epitope mapping by photobleaching fluorescence resonance energy transfer measurements using a laser scanning microscope system. *Biophysical Journal*, 61(3):661 – 670, 1992.

A LabView program operation

The LabView program PMT_out_vs_gain.vi was developed in order to speed up the measuring process of the setup by automatizing the DC power supply and by performing some basic data analysis on the output voltage of the PMT. It was designed to measure the output voltage of the PMT as a function of the control voltage, so it is mostly useful for the calibration of the setup and for background measurements. Measurements with a single control voltage setting such as photobleaching measurements can be done with this virtual instrument, but one could as well use DAQExpress^{TM} as it is more convenient for this type of application. In this appendix, we will explain how the program PMT_out_vs_gain.vi works and how to use it.

A.1 Description of the front panel and block diagram

As in all LabView programs, the PMT_out_vs_gain.vi virtual instrument is composed of a front panel, which is the interface through which the user can easily change the parameters of the measurement and run the program, and a block diagram, which contains the graphical code of the program.

The front panel of the program is shown in Figure A.1. The first dialog box allows the user to enter the full path to the working directory of the program, in which the output files containing the results of the measurements will be created. The other input to be defined by the user are the numerical values of the control voltage settings, and of the data acquisition settings. In order to perform recording of the output voltage of the PMT for different values of the control voltage, the program features a loop in control voltage as we can see in the block diagram in Figure A.4. This loop starts at 0.5V and has user-defined step and upper value, which are to be entered in the "Control voltage step" and in the "Control voltage stop" dialog boxes respectively. The last input values to be defined by the user are the rate of the data acquisition, in samples per second, to be entered under "rate" and the acquisition time in seconds, under "Acquisition time (s)". The other features that are on this control panel are indicators and allow the user to monitor the measurements while the program is running. The Waveform Graph displays the data points after each iterations of the program and the mean value of the output signal is displayed in the "Voltage" indicator. The "Control voltage" indicator displays the control voltage corresponding to the program's last iteration, for which the output signal and its mean value are displayed. The last indicator just shows the total number of iterations under "Number of measurements".

Looking at the example settings that are shown in Figure A.1, we can see that an upper value of 1V and a step of 0.05V were chosen by the user, corresponding to 11 different values of the control voltage for each of which the output signal of the PMT was recorded for 0.1s at a sampling rate of 10000 samples per second, that is a thousand data points.

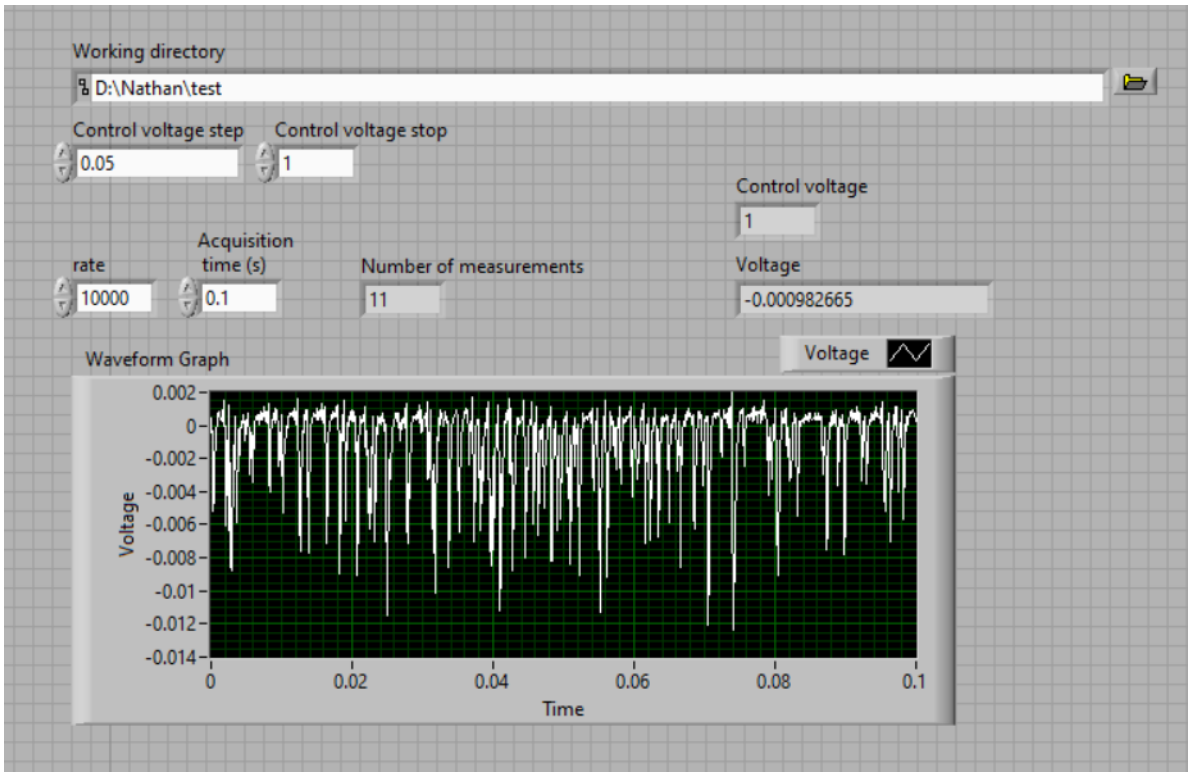

Figure A.1: Front panel of PMT_out_vs_gain.vi.

If we look at the block diagram (Figures A.2 to A.4), we can see that it is organized in two sequences, the first one on the left contains all the initialisation operations, which are reading the inputs, creating the output files and initializing the Dc power supply, and a second sequence containing the loop changing the control voltage, performing the data acquisition and saving the data to the output files.

Let's first look at Figure A.2 which shows a part of the initialization sequence, on the top left of the block diagram. This part of the diagram contains the reading of the inputs from the numerical controls of the front panel and calculates the number of measurements that is then passed on to the other sequence to determine the number of iterations of the loop shown in Figure A.4. It also contains the reading of the path to the working directory and the creation or replacement of the output files. This program creates two output files : the first one, named log.txt, contains all the data recorded by the DAQ during this run of the program and the second one, outvsgain.txt, features three columns containing the control voltage and the corresponding mean value and standard deviation of the output voltage. it is important to note that since the program creates or replaces the output files, the user has to either rename the files or change working directory between each run of the program in order to not lose previously acquired data.

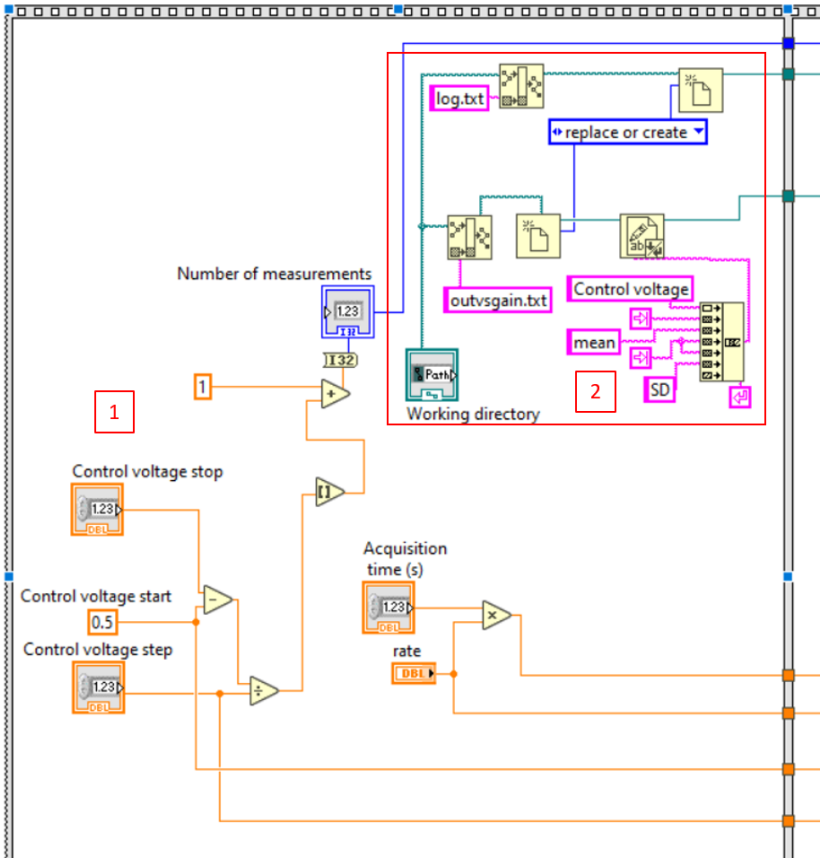

Figure A.2: Part of the block diagram showing the reading of the inputs and the calculation of the number of measurements (1) as well as the creation or replacement of the output files (2)

The second part of the initialization sequence is displayed in Figure A.3. Its role is to initialize the settings of the DC power supply. First it selects the output 1 channel of the power supply and sets the voltage to +5V, corresponding to the low voltage input of the PMT. Then the output voltage of the second channel is initialized to 0.5V, which is the starting value of the control voltage. It is important to note that the control voltage should not exceed 1.1V, therefore the user has to make sure that the low voltage input of the PMT is plugged into the output 1 of the power supply and the control voltage input is plugged into the Output 2 in order to not damage the PMT.

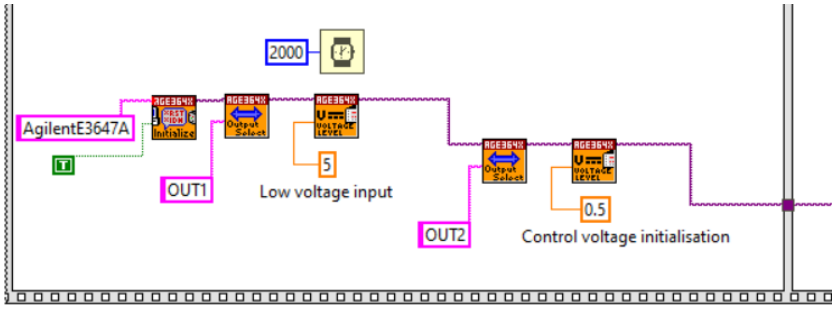

Figure A.3: Part of the block diagram in which the power supply is initialized

The second sequence of the program that is shown in Figure A.4 is composed of a for loop in which all the operations are performed. These operations can be grouped in four main tasks : acquiring the data, setting the control voltage, writing the data to the output files and checking that the output voltage of the PMT doesn't reach a too high level.

Before entering the loop, the program enables the power supply output, which is disabled by default. Then, for each iteration of the loop, the program calculates the control voltage by multiplying the step defined by the user by the loop index ((part of the block diagram labeled (3) in Figure A.4). This value is then applied to the output 2 of the power supply.

The data acquisition sequence (part of the block diagram labeled (2) in Figure A.4) is the part of the program that controls the DAQ via the DAQ assistant function, which takes as input the rate of measurements and the number of samples to be recorded, that is calculated by the program based on the acquisition time defined by the user. As we can see from the block diagram, before each call of the DAQ assistant function, the program waits for 1.5s. The reason for this pause in the data acquisition is that the output voltage from the PMT takes some time to stabilize upon changing the control voltage. Therefore, in order to have a signal that is as stable as possible for the whole duration of the measurement, the program has to wait for some time after the control voltage is modified. The specific value of 1500 ms was roughly determined by trial and error and it could be over-evaluated. A more in-depth study of the PMT gain upon changing the control voltage would be required to optimize the waiting time.

The output of the DAQ assistant, formatted as dynamic data, is then sent to the function that displays the waveform graph on the control panel and to the section where the program checks that the signal doesn't reach a voltage too high (part of the block diagram labeled (5) in Figure A.4). The maximum voltage was set to 10V in order to make sure that the PMT is not damaged while running the program. If the voltage recorded by the DAQ exceeds 10V, the program stops, the output of the DC power supply is disabled and an error message is displayed.

In the last part of the block diagram (labeled (4) in Figure A.4), the dynamic data acquired by the DAQ is converted to an array of which the mean value and standard deviation is then computed. The resulting data is finally written to the output files.

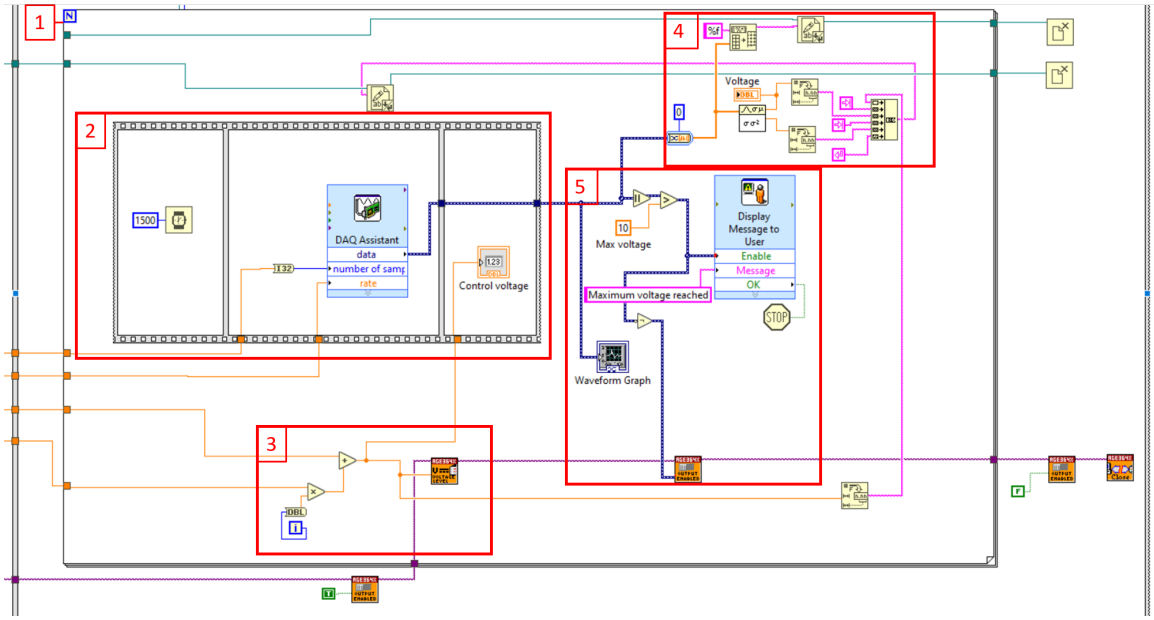

Figure A.4: Part of the block diagram showing the sequence of the program in which the data is acquired and saved. (1) for loop (2) data acquisition sequence (3) control voltage setting (4) writing to output files (5) program stopping in case of too high output voltage from the PMT

A.2 Running the program on a new system

The program PMT_out_vs_gain.vi requires the driver for the agilent E364xA series DC power supply to be installed on the computer. As a first step, the user should therefore download the driver from the National Instruments website and install it. Once the driver is installed, another step is required for the program to work properly, which is to make sure that the instrument's VISA alias on the system is the same as the one the program uses. In order to do that, one has to open the National Instruments Measurement & Automation Explorer software and select the DC power supply, which should appear as an instrument connected via serial port under "Devices and Interfaces", as shown in figure A.5. If the power supply is not showing, one should make sure that it is properly connected and that the driver is installed.

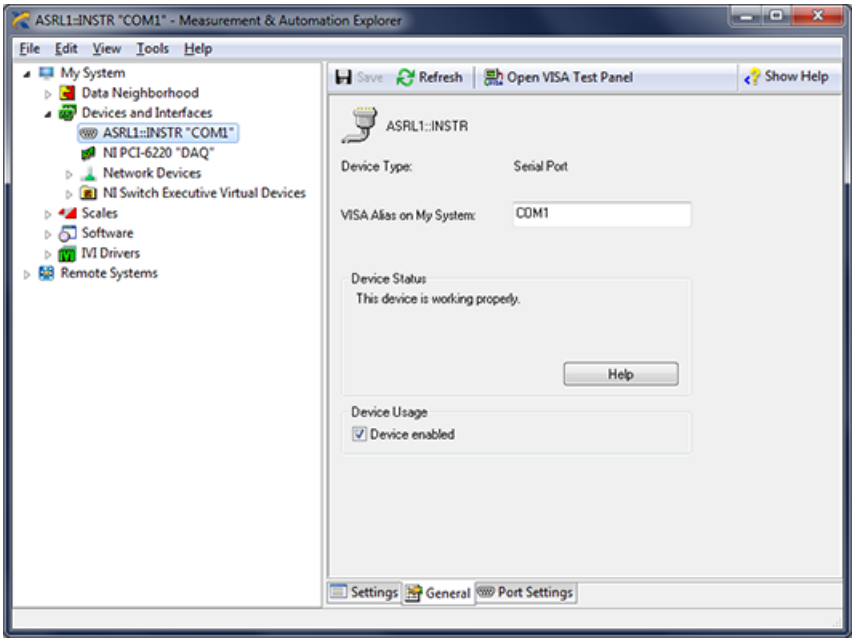

Figure A.5: Configuration window of a serial port instrument in the Measurement & Automation Explorer

Then one has to change the VISA Alias of the instrument in order to match the alias that is used by the Initialize function in the LabView program's block diagram which is "AgilentE3647A" as shown in figure A.6. Once this is done, save changes and close the Measurement & Automation Explorer and the program is ready to run.

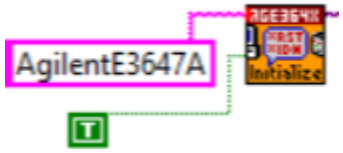

Figure A.6: Part of the PMT_out_vs_gain.vi LabView program's block diagram showing the function initializing the agilent DC power supply, which takes the VISA Alias of the instrument as an input.